Subduction Ground Motions Characterization and Their Relation to Potential Structural Damage

Carlos E. Ventura[1], Ilaria Capraro[2], Yuxin Pan[3], Michael Fairhurst[2], Armin Bebamzadeh[3], Marisa J. Mulder[4]

[1] Professor, Department of Civil Engineering, The University of British Columbia - Vancouver, BC, Canada.
[2] Research Assistant, Department of Civil Engineering, The University of British Columbia - Vancouver, BC, Canada.
[3] Research Associate, Department of Civil Engineering, The University of British Columbia - Vancouver, BC, Canada
[4] Former Research Assistant, Department of Civil Engineering, The University of British Columbia - Vancouver, BC, Canada, now, Design Engineer at Fast + Epp, Vancouver, BC, Canada

ABSTRACT

The damage caused by large subduction earthquakes is due in part to high number of load reversal cycles. Experimental and analytical studies indicate that shaking duration and number of cycles contribute to the damage. Furthermore, in recent years, the strong ground motion subduction records database has significantly expanded, mostly as a consequence of the latest subduction events in Chile and Japan. Engineers are facing many challenges in dealing with these particular records, mainly associated to methods for selection and scaling of the motions to use as input for dynamic structural analysis. One of the aspects which has not been thoroughly investigated is the link between strong motions observations from recordings and their relationship with the observed damage. This is particularly evident from field observations of damage to structures in the vicinity of sites with strong motion instruments during the Chile 2010 El Maule and the Japan 2011 Tohoku earthquakes. The data acquired at some of these sites showed very significant levels of intensity and duration of ground shaking, yet the damage observed in the area was insignificant and not what was expected, while there was significant damage at other sites with lower levels of ground shaking.

This paper discusses the results of recent investigations conducted by the authors on how to correlate damage with ground motions shaking and duration from subduction earthquakes. It also investigates how shaking duration affects the response of buildings, with emphasis on concrete and wood frame buildings in British Columbia, which is located in the Cascadia Subduction Zone. Fragility curves for collapse due to subduction ground motions are compared with those from shorter duration events in order to illustrate how the probability of collapse is affected by long duration shaking for different structural systems.

Keywords: Subduction earthquakes, long duration ground motion, damage index, fragility curve, wood frame buildings, RC concrete shear wall buildings.

1. INTRODUCTION

Significant megathrust earthquakes since 2004 in Sumatra, Indonesia (M_w 9.1, 2004), El Maule, Chile (M_w 8.8, 2010), and Tohoku, Japan (M_w 9.0, 2011) have served as reminders that large magnitude, long duration earthquakes are possible in subduction zones around the world. Reconnaissance teams have repeatedly reported large levels of damage from these events, due in part to the high number of load reversal cycles. Additionally, many experimental tests indicate that load duration and number of cycles are highly important to the observed damage. Most studies using numerical models of structures also agree that ground motion duration is of significant importance when considering cumulative damage measures. However, currently, no such provisions for shaking duration are required in most building and bridge codes. This may be in part due to the conflicting results of studies which consider the effect of ground motion duration on peak structural response (drift or displacement), and some of those conclude that duration of shaking is important, while others concluded the opposite.

Currently, the effect of ground motion duration on the damage or collapse probability of structures is not well established. This is in part due to different conclusions reached by researchers studying ground motion duration or number of cycles using observational evidence, experimental testing, and numerical modeling. Some studies have observed greater damage caused by the rapid energy release in short duration crustal events, while others suggest that the large number of cycles from subduction interface events cause greater damage.

Southwestern British Columbia is a region characterized by a very complex tectonic environment. Contribution to the seismic hazard is given by three different types of seismic sources: crustal, subcrustal and subduction earthquakes. While crustal and subcrustal earthquakes are usually characterized by low/intermediate magnitudes and short durations, subduction earthquakes are associated with larger magnitudes and longer duration of shaking. Because of the proximity of two major cities in Canada (Victoria and Vancouver) to the Cascadia Subduction Zone, it is of interest to study the effects of subduction ground motions on the seismic performance of structural systems. Subduction ground motions are important for Western Canada and their effects on the response of structures needs to be investigated in detail. This paper summarizes results of recent studies conducted by the authors and provide insight into subduction earthquakes by carrying out a comprehensive analysis of ground motions recorded during this type of event. The effects of duration and long period components of the ground motions on the linear and nonlinear response of wood and shear-wall concrete structures will be discussed.

2. CHARACTERISTICS OF SUBDUCTION GROUND MOTIONS

Long duration subduction ground motions

Current building code designs are based on design spectra that provide spectral acceleration as a function of the building period. However, acceleration spectra do not reflect adequately the effects of long duration motions. Long duration is, among other aspects, a unique characteristic that differentiates subduction ground motions from the other earthquake motions.

Long duration of shaking consists of frequency components that are repeated for many cycles. This, in turn, might lead to resonant-like response of structures with the same frequency (or period) as the ground motion. The effect on many cycles of frequency components that have significant contribution to the ground shaking on the associated response spectra will be seen a sharp peaks of high spectral values at those frequencies. One might erroneously conclude that systems with such frequency might experience large demands, hence damage. The effect of a large number of motion cycles dominated by a certain frequency can be better understood by reference to the response of a Single-Degree-of-Freedom (SDOF) system to sinusoidal excitation of limited number of cycles. In order to understand the effect of large number of cycles of motion dominated by a certain frequency, a study on the response of a SDOF systems to sinusoidal excitation with limited number of cycles was conducted.

To help understand this, response spectra of simple sinusoidal signals are computed by increasing the number of cycles of the excitation. Response spectra are calculated for sinusoidal signals with a period of 1 sec, peak acceleration of 0.2 g and 5% damping ($\xi = 5\%$). Figure 2.1, 2.2 and 2.3 show the spectra for acceleration, velocity and displacement, respectively. Seven sinusoidal signals of 1, 2, 3, 4, 5, 10 and 300 cycles are considered, and their response spectrum is plotted for comparison in Figures 2.1 to 2.3.
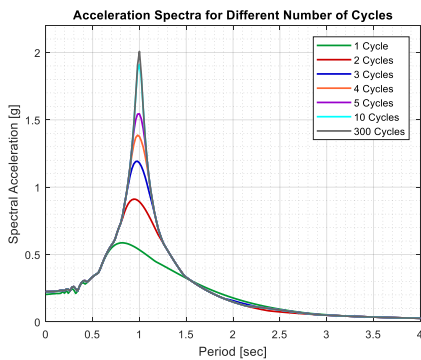

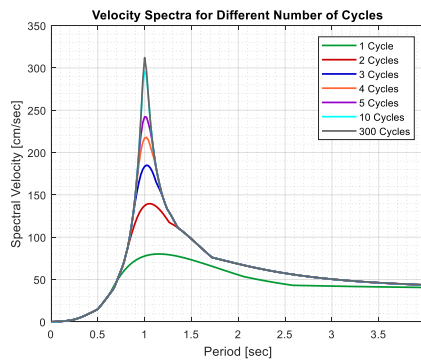*Figure 2.1: Acceleration response spectra of sinusoidal signals with varying number of cycles ($\xi = 5\%$).*

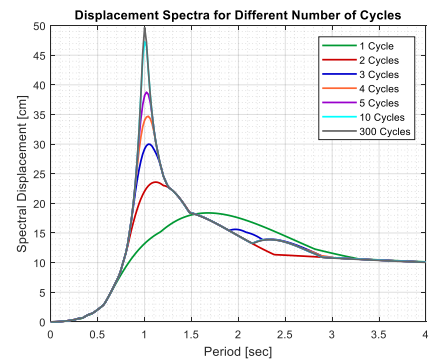*Figure 2.2: Velocity response spectra of sinusoidal signals with varying number of cycles ($\xi = 5\%$).*

Figure 3.3: Displacement response spectra of sinusoidal signals with varying number of cycles ($\xi = 5\%$).

As the number of cycles increases, the spectral amplitude at resonance becomes progressively larger. Eventually, after 10 cycles of motion, the response spectrum of the sinusoidal signal will be the same as the 300 cycles spectrum. This example clearly shows that the duration of the signal is well represented, up to 10 loading cycles, at structural periods close to resonance. The same can be seen from the velocity and displacement elastic response spectra.

The sharp peaks due to the repetition of many loading cycles with the same frequency can be observed also in response spectra generated using subduction ground motion records. This is in contrast to the traditional belief that large magnitude earthquakes at long distance from the site would commonly generate a flatter spectrum at short period and larger amplitudes at longer periods [1]. An example is provided in Figure 2.4, which shows the acceleration response spectra from the Tsukidate station (Japan) during the 2011 Tohoku earthquake. At a period of 0.24 sec, the spectrum shows a very sharp peak and is associated

with a large spectral amplitude of 13 g. The repetition of many short-period cycles (period of about 0.24 sec) resulted in a spectrum with high demands in the low-period range.
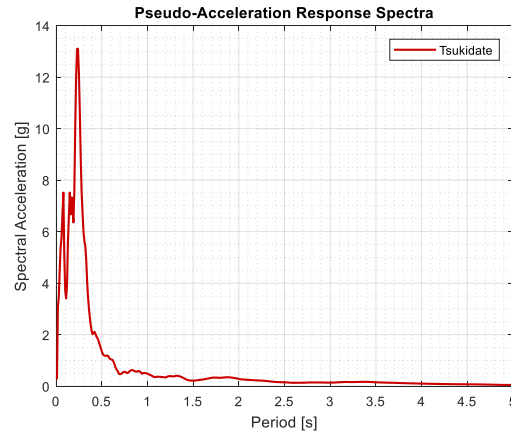

Figure 2.4: Acceleration response spectra at Tsukidate station (MYG004) during the 2011 Tohoku earthquake.

In the last few years, three major studies have been conducted to evaluate the effect of long duration ground motions on the seismic performance against collapse of a variety of structural systems [2, 3, 4]. These investigations clearly showed that the demands imposed on the structures are significantly higher when considering long duration motions compared to the ones obtained with shorter duration motions, thus leading to higher probabilities of collapse. Moreover, these studies not only demonstrated the importance of the effects of long duration shaking, but also that these effects are more important for structures characterized by severe stiffness and strength degradation. Post-earthquake field investigations confirm that structural damage from subduction earthquake shaking is not always directly correlated only to seismic intensity and duration, but is also dependent on the building type, building natural period and the dominant periods of the ground motion.

Characteristics and consequences of past earthquakes events

The Michoacán Earthquake, which hit Mexico in 1985, was a M_w 8.1 subduction earthquake with a duration of minutes. This event caused amplification of the horizontal components of motion in the period range 2-3s in the area of Mexico City underlain by soft lake sediments [5]. Extensive damage was caused by resonance between the 2 sec period of the lake sediments and buildings characterized by a similar fundamental period [6]. In addition, in the lake bed basin the duration increased due to the waves being reflected back and forth from the walls of the basin. The main finding from the Michoacán Earthquake was the significant impact of the soil conditions in both the amplification and duration of the ground shaking and the magnifying effects on the dynamic response of moderate period structures.

Nineteen years later on December 26th, 2004 the Sumatra-Andaman Earthquake occurred where the Indian and Australian plates subduct beneath the Sunda plate. With a 1300-1500 km long fault and a rupture duration of 500 seconds, the Sumatra Andaman earthquake was assigned as a moment magnitude M_w 9.1-9.3 event [7]. In the coastal region of Banda Aceh the main type of construction were low-rise timber frame buildings and non-engineered RC buildings with unreinforced masonry infill walls [8]. Although the low-rise timber buildings survived the ground shaking, they collapsed under the water pressure of the tsunami waves [9]. Non-engineered RC buildings suffered total or partial collapse because of the lack of ductile detailing and poor seismic design. Unreinforced Masonry (URM) walls were used as infills for the RC frame structures and experienced out-of-plane failures due to the wave pressure of the tsunami. Post-earthquake field investigations were also conducted in Port Blair, capital of the Andaman and Nicobar Islands. Low-rise traditional timber and masonry structures performed very well during the earthquake shaking. Interestingly, an old mosque built in 1913 with masonry domes and minarets and retrofitted in 2001-2002 did not suffer any structural damage, except the collapse of few slender minarets. On the other hand, several low-rise RC frames experienced substantial damage during the earthquake. As in the case for Banda Aceh, the structural damage was mostly attributed to poor construction and lack of ductile detailing [10].

On February 27th 2010, the M_w 8.8 Maule earthquake occurred in central Chile. With a rupture area of 81,500 km^2, it affected a vast region of the country. Besides the failure of a few engineered buildings caused by structural irregularities and limited ductility capacity, reconnaissance teams reported that the performance of engineered buildings in Santiago was quite good. Masonry construction in the Maule region suffered the most damage. In the city of Talca, 80% of the buildings were damaged and 50% were slated for demolition. The variable damage distribution patterns were attributed in part to local site conditions [11]. At Curico and three other locations (Maipu, Concepción and Melipilla) the recorded motions resulted in seismic demands exceeding the design spectra [12]. In the city of Curico, 90% of the adobe construction was destroyed and structural damage was observed also in hospitals, schools and churches.

The 2011 Tohoku Earthquake off the Sanriku coastline in Japan was a M_w 9.1 event and has been ranked as the 4th largest event ever in terms of magnitude [13]. Japan has a long history of large magnitude earthquakes, but when the Tohoku earthquake hit Japan, the consequences in terms of scale of earthquake, tsunami's height, flooding extension, human and economic losses, greatly exceeded any expectations. The fault rupture of the Tohoku involved three different segments in sequence, resulting in a maximum slip of about 40 m and a significant amount of energy released in a three-minute span. These characteristics made the earthquake not only powerful, but also extremely long in duration. As a proof that the event was beyond any expectations of the authorities, the recording capacity of several seismographs was exceeded and therefore the data stored was partially incomplete [14].

Far away from the epicenter, at Tokyo and Osaka Bay stations, the recordings showed long period ground motions [15]. The effects of long period motions were different depending on the location and structures involved. For instance, it was found that a 37 storey RC building in Tokyo experienced a maximum displacement at the top of about 17 cm, while the ground displacement was 20 cm. On the other hand, a 55 storey steel building in the Osaka Bay area which was 770 km distant from the epicenter, showed a zero-to-peak maximum displacement at the top floor of more than 130 cm, while at ground level, the maximum displacement observed was less than 10 cm. This means that, in one single cycle of vibration, the building experienced a total amplitude of about 260 cm [15]. The tall building in Osaka showed resonance between the fundamental natural period of the building (around 6.5-7.0 seconds) with the predominant period of the ground motion (6-7 sec). The extraordinary long duration of the shaking subjected structural systems to several cycles of deformation. A direct observation of this phenomena is given by records obtained from an instrumented 9-storey shear wall building in Tokyo, which made it possible to track the change in its fundamental period every 10 seconds. Before the earthquake hit, the first natural period was estimated to be 0.7 sec in both principal directions. During the shaking, due to the progress of damage and flexural failure in members and connections, the period increased to 1 sec during the first wave and then from 1.2 to 1.5 sec during the second wave. As a result, the fundamental natural period was elongated to twice the initial period and the stiffness was reduced by a factor of 4 [15].

3. DAMAGE POTENTIAL OF SUBDUCTION GROUND MOTIONS

After recent large magnitude subduction events (2011 Tohoku and 2010 Maule earthquakes), engineers and seismologists conducted extensive post-earthquake field investigations with the goal of collecting valuable technical data and developing a better understanding of the structural damage associated with subduction earthquakes. These investigations showed how structural damage from earthquake shaking is not always directly correlated to seismic intensity, but is also dependent on the building type and the dominant periods of the ground motion. This Section presents an exploratory study about the damage potential of subduction earthquakes with the aim to identify ground motion parameters which would better relate to the damage observed during post-earthquake field investigations.

A striking example is given by the field evidence at Sendai and Tsukidate stations during the 2011 Tohoku Earthquake. According to the JMA [16] intensity scale, the maximum seismic intensity was 7 in the city of Kurihara (K-NET Tsukidate) and the rating in Sendai was 6+ [17]. As shown in Figure 3.5, both sites are at comparable distances from the rupture [15]. A Peak Ground Acceleration (PGA) of 3.0 g was recorded in Tsukidate (MYG004), while at Sendai (MYG013) the PGA was 1.5 g. Despite this extremely large difference in PGA, the damage was much greater in Sendai than in Tsukidate, confirming that the PGA is not a good index of damage potential. Similar consideration holds for the Peak Ground Velocity (PGV). While the PGV at Tsukidate reached 110 cm/sec, the PGV intensity in Sendai was of about 86 cm/sec. The maximum displacement (PGD) were roughly 22 cm at both stations. Neither the PGV, nor the PGD provided useful information about the damage observed at the site.
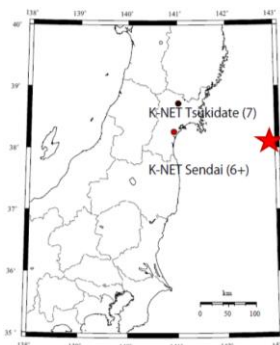

Figure 3.5. Location of the Tohoku epicenter and the stations of Tsukidate and Sendai

Post-earthquake field observations

Limited damage was observed in wood houses in Tsukidate, but it was not as severe as expected given the high JMA seismic intensity rating. In some cases, where the damage was substantial, it was caused by ground liquefaction and soil failure and was not directly related to poor structural performance under ground shaking. Figure3.2 shows an example of damage in Tsukidate, where the objects on the cupboard overturned during the shaking. On the other hand, the containers shown in Figures 3.3 and 3.4 with high aspect ratios did not overturn despite the very high acceleration.

In the city of Sendai, significant damage was observed in wooden houses. Reinforced concrete buildings suffered severe damage as well. Post-earthquake evaluations reported several types of damage patterns in reinforced concrete buildings. An example of mid-storey collapse in a reinforced concrete building is shown in Figure3.5. Damage in terms of shear failure was observed also in first storey columns of a low rise building. Figure3.6 shows shear cracks on the columns. Damage in boundary beams was reported as well in shear wall buildings [15]. Figure 3.7.7 shows an example of 8-story shear wall building where significant damage was localized around the openings in the coupling beams.
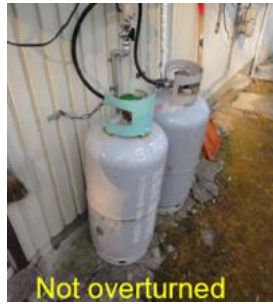

Figure3.2. Overturned objects in Tsukidate [15].

Figure3.3. Not overturned objects in Tsukidate [15].

Figure 3.4. Not overturned objects in Tsukidate [15].

Figure 3.5. Collapse of a mid-story of a reinforced concrete building in Sendai [15].

Figure 3.6. 1st storey shear cracks of column in Sendai [15].

Figure 3.7. Damaged boundary beams with openings [15].

Ground motions parameters and structural damage

A detailed study was conducted to explain the difference in damage potential of the two site records by examining the different ways of characterizing ground motion intensity. The ground motion records for Tsukidate and Sendai were obtained from the Japanese Kyoshin networks K-NET and KiK-net database of the National Research Institute for Earth Science and Disaster Prevention [18]. The main direction of the acceleration motion is the North-South (NS). For this reason, the investigation about the damage potential at the two stations was carried out considering the NS component.

It is well recognized that PGA is a poor indicator of damage potential: PGA was 3.0g in Tsukidate and only half as large at Sendai at 1.5 g, yet Sendai had much greater damage. In addition to the traditional ground motion parameters, such as PGA, PGV and maximum displacement, attention was focused on the frequency content and the significant duration. Significant duration is defined as the time from 5% to 95% of the Arias Intensity and it is traditionally designated as D_{5-95}.

Table 2-2 provides a summary of the main characteristics of the motions recorded at Tsukidate and Sendai stations. It can be noted that although the PGV at Tsukidate is higher (110 cm/sec) than at Sendai (86 cm/sec), much more damage was observed at Sendai. The maximum ground displacements were similar at about 22 cm for both stations. It appears clear that peak ground parameters do not reflect adequately the damage potential of ground motions. From a qualitative point of view, both records

have similar time histories, which can be described by two-wave groups as shown in Figure . One of the characteristics of the records which underlines the different nature of the ground motions is the frequency content (Figure 3.93.9). Tsukidate motions have a much higher frequency content, with higher amplitudes at short periods (about 0.2 sec), while the motion at Sendai generates a much wider frequency spectrum within the period range 0.5 and 1.0 sec. The significant duration at Sendai is about 89 sec, while the motion at Tsukidate has a duration of 80 sec. It seems unlikely that the small difference (about 10%) in duration would explain the much greater and widespread damage in Sendai respect to Tsukidate.

The Arias Intensities of Tsukidate and Sendai are shown in Figure 3.10. It is clear that the Arias intensity for Sendai is only a small fraction of the Arias Intensity of the Tsukidate record. However, the damage in Sendai was much greater than the damage in Tsukidate, despite the fact that the Arias Intensity is supposed to be a measure of the energy in the ground shaking. Clearly, the Arias Intensity is not in this case a good measure of potential damage to structures.

Table 1. Summary of the characteristics of the motions at Tsukidate and Sendai.

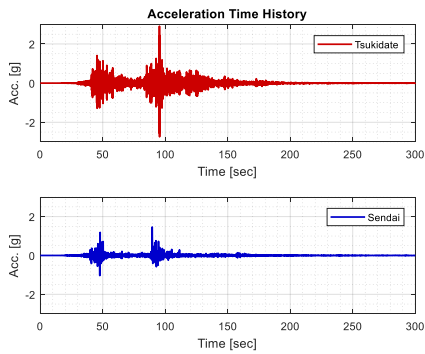|	**Tsukidate**	**Sendai**
Record Name	MYG0041103111446-NS	MYG0131103111446-NS
JMA Seismic Intensity	7	6+
Max. Acceleration	2.91 g	1.46 g
Max. Velocity	110 cm/sec	86 cm/sec
Max. Displacement	22.5 cm	22.4 cm
Waveform	2-wave groups	2-wave groups
Period (Frequency)	Short Period 0.2 sec (5 Hz)	Intermediate period 0.5 – 1.0 sec (1 – 2 Hz)
D_{5-95}	80.85 sec	89.72 sec

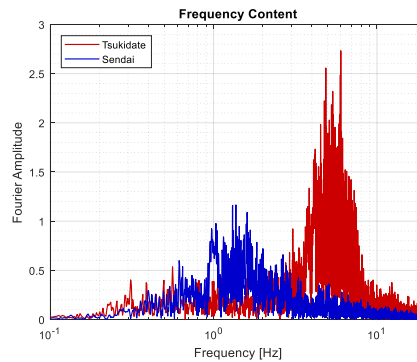*Figure 3.8. Comparison of time histories at Tsukidate (red) and Sendai (blue).*

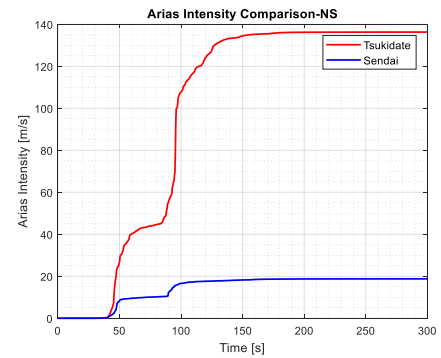*Figure 3.9. Comparison of frequency contents at Tsukidate (red) and Sendai (blue).*

Figure 3.10. Comparison of Arias intensities at Tsukidate (red) and Sendai (blue).

Elastic response spectra analysis

The use of the elastic response spectrum as an index of damage potential is investigated. This is a logical assumption because the elastic spectrum is commonly used as the basis for design in current building code provisions. Elastic response spectra for pseudo acceleration (PSA), pseudo velocity (PSV) and spectral displacements have been calculated and plotted for both sites as showed respectively in Figure 6. The motion recorded in Tsukidate is associated with a spectral shape featuring a very sharp spike at 0.24 sec in the acceleration response spectrum with the maximum response reaching 13 g and much lower amplitudes at other spectral periods. The high peak ground acceleration of about 3 g recorded in Tsukidate resulted from a single pulse with high frequency components. There is very little impulse associated with the spike and therefore is not capable of driving the system to significant displacements. This was very evident in the subsequent dynamic analysis presented below where the responses reversed very quickly and the displacements were quite insignificant. On the other hand, the spectrum associated to the motion recorded in Sendai shows significantly lower amplitudes but features a broader spectral shape. It should be noted that, although much less than the peak spectral acceleration at Tsukidate, these amplitudes are still significant at about 1.7 g over a fairly broader period range from 0.1 to 5.0 sec.

The difference in velocity and displacement spectra supports the greater damage observed at Sendai. This is particularly evident in the period range of 0.4 to 2 sec (Figure 7), where the Sendai velocity and displacement spectra are much greater than the Tsukidate spectrum and therefore imparts greater energy to the system. This is supported by post-earthquake field observations

which reported significant damage in low and intermediate period buildings in the Sendai area. A similar observation can be made about the elastic displacement response. As shown in Figure 3.13 the motion at Sendai generates higher displacement demands than at Tsukidate in a period range from 0.5 to 3 sec.
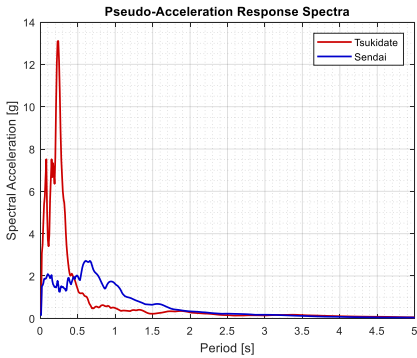

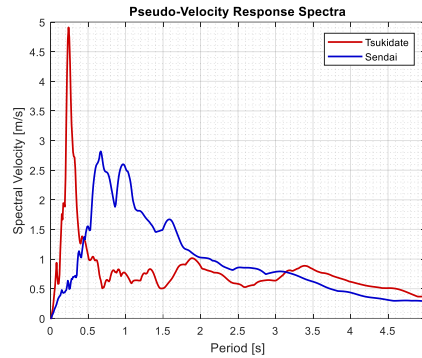*Figure 6. Elastic pseudo-acceleration response spectra for Tsukidate and Sendai (ξ = 5%).*

Figure 7.12. Elastic pseudo-velocity response spectra for Tsukidate and Sendai (ξ = 5%).

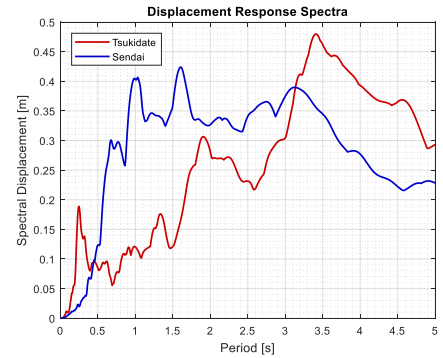*Figure 3.13. Elastic displacement response spectra for Tsukidate and Sendai (ξ = 5%).*

Constant ductility spectra analysis

The Constant ductility spectrum is a tool used to calculate the lateral resistance of a system to ensure that a target ductility is achieved in design [19]. Constant Ductility spectra have been calculated for Tsukidate and Sendai using the Bispec V2 computer program [20]. These spectra have been generated considering the Bilinear Plastic Model implemented in Bispec. The bilinear system is characterized by a linear behavior up to the yield limit and then exhibit a softer post-yield response, characterized by a hardening stiffness ratio (post-yielding stiffness/elastic stiffness) equal to 0.05. The spectra were obtained considering a damping ratio equal to 5%. Different levels of ductility (1.5, 2 and 3) were analyzed.

Figure 3.14 show the constant ductility acceleration spectra for Tsukidate and Sendai, respectively. The nonlinear spectra for the motions recorded in Tsukidate show how the spectral shape significantly changes for each level of ductility when considering a nonlinear system. This rapid decrease in spectral amplitudes is particularly significant in comparison with the very sharp peak at the period of 0.24 sec. A slight increase of ductility to 1.5, results in a decrease of about 60% in spectral amplitude, reaching a spectral acceleration of about 5 g, much less than the elastic spectral value of 13 g. This shows that even a small amount of inelastic behavior would reduce high intensity short period peaks to significantly lower values. As for the inelastic spectra generated with the Sendai record, the spectral ordinates decrease in amplitudes (up to 40%).

In general, it can be seen that the displacement demands of the Sendai motion are greater than the demands at Tsukidate for a period range from 0.4 to 3.3 sec, for the ductility capacities under consideration. Based on the results shown in Figure 8, it would seem that the constant ductility displacement spectra may be a useful tool for discriminating between the damage potential of the different earthquake records.
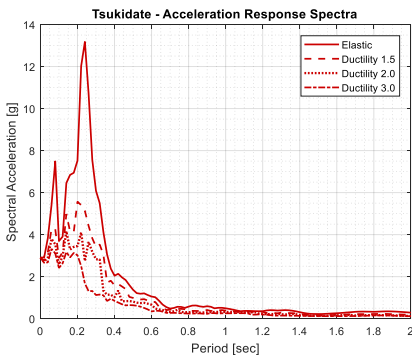

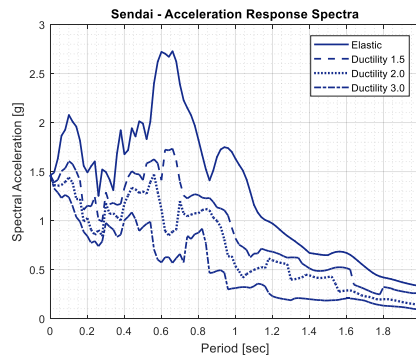*Figure 3.14. Constant ductility spectra for Tsukidate (ξ = 5%).*

Figure 3.15. Constant ductility spectra for Sendai (ξ = 5%).

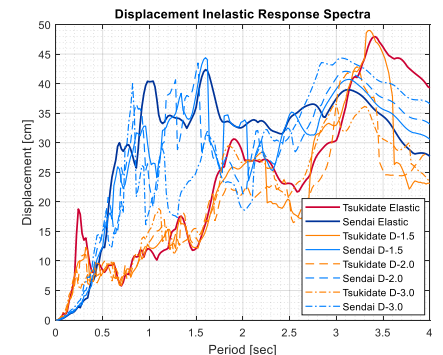*Figure 8. Constant ductility spectra for displacement response (ξ = 5%).*

The rapid decrease in spectral amplitudes at period of 0.24 sec observed in the constant-ductility spectra generated with the motion in Tsukidate can be explained by considering the inelastic spectra of a simple sinusoidal signal (Figure 3.17.17). The sinusoidal signal considered has an acceleration amplitude of 0.2 g and a period equal to 1.0 sec. The constant ductility spectra has been generated for acceleration and is shown in Figure 3.183.18. The ductility values considered for analysis are 1.5, 2.0 and 3.0. The elastic spectrum is plotted for comparison. It can be observed that when the structural period is in resonance with the period of the signal, a similar drop in amplitude occurs for three ductility levels. For instance, when the ductility capacity of the system is 1.5, the inelastic acceleration amplitude at resonance decreases to about 25% of the elastic response. This trend is clearly reflected in the constant-ductility spectra presented in Figure 3.14, confirming what previously observed in the Fourier spectrum: the record at Tsukidate is characterized by the repetition of loading cycles of period about 0.2 sec.
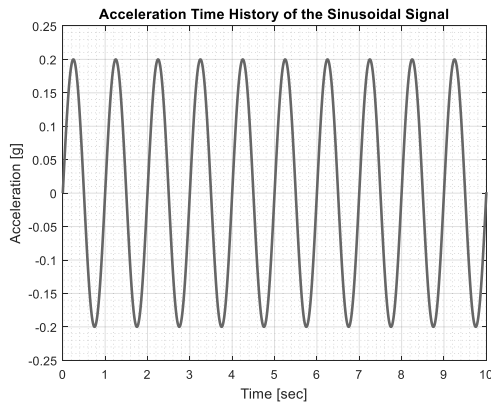
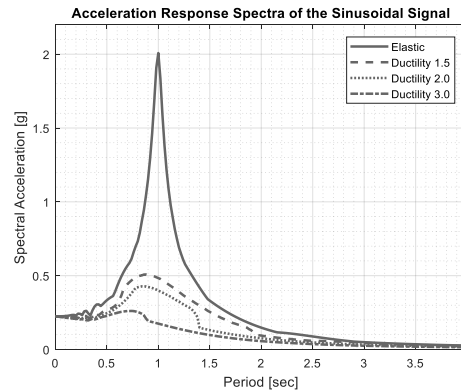*Figure 3.17. Acceleration time history of a simple sinusoidal signal.*

Figure 3.18. Acceleration response spectra of the sinusoidal signal for different ductilities (ξ = 5%).

Insight from nonlinear response

A number of nonlinear time history analyses were performed using the Bispec V2 computer program [20]. The structural models were represented by SDOF systems with fundamental periods of 0.2 and 1.0 sec to represent short and intermediate period structures. The material models selected for analyses were the Bilinear and Clough models with no limitation on the ductility capacity. Unlike the Bilinear model, the Clough model is a hysteretic model that exhibits a degraded stiffness during unloading which is dependent on the current state of the model and on the largest displacement previously reach in each direction. This stiffness change occurs when the system force crosses the zero force line [20, 21]. As in the case for the constant ductility spectra, the hardening stiffness ratio consider for analysis was 0.05. The damping ratio ξ was equal to 5%.

The input motions were the recorded Tsukidate and Sendai records. For each analysis, displacement response time history, yielding events time history and force-displacement hysteretic loops were plotted for comparison. Results of these analyses are presented in Figure 9 to Figure 16.26. The results at Tsukidate are shown in red, while Sendai results are shown in blue.

For a short period structure (0.2 sec) represented by a Bilinear model, the number of yielding events generated by the motion at Tsukidate is much higher than at Sendai (Figure 9). On the other hand, the maximum displacement response associated with Tsukidate record is lower than the one in Sendai (3.20). The analysis of an intermediate period structure (1.0 sec) using the same material model results in more yielding episodes in Sendai (Figure 11) and the displacements are higher (3.22). The motion at Tsukidate, even though it generates more yielding events at short periods, does not push the system as far as into the inelastic range as the motion recorded at Sendai. Similar results were found using a nonlinear Clough-type material model (Figure 133.23 to Figure 16), with the exception that at short period (0.2 sec), the motion at Sendai generates not only larger deformations, but also a greater number of yielding cycles than at Tsukidate (Figure 13 and 3.24).

Nonlinear analysis allows the evaluation of the nonlinear displacement demands that a particular structural system is expected to withstand during an earthquake. Therefore, nonlinear analysis of simple systems can give useful insights into damage potential.
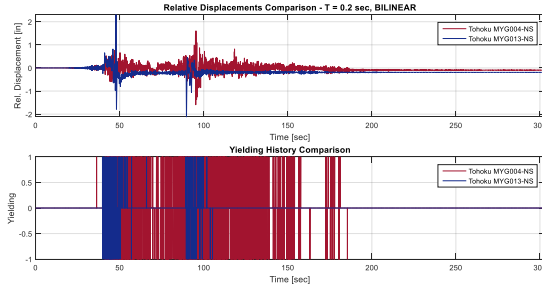
Figure 9.19. Acceleration and yielding time history for Bilinear SDOF at 0.2 sec.
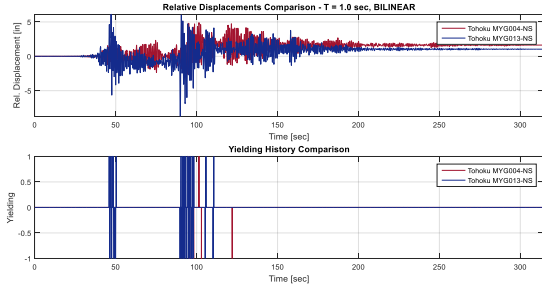

Figure 10. Hysteresis loop for Bilinear SDOF at 0.2 sec.

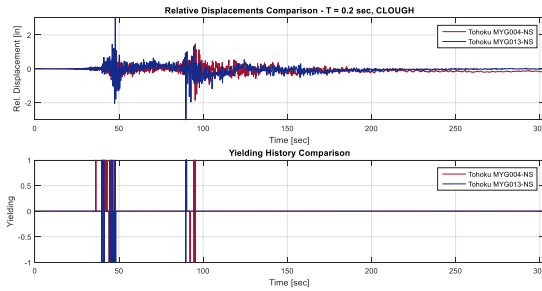*Figure 111. Acceleration and yielding time history for Bilinear SDOF at 1.0 sec.*

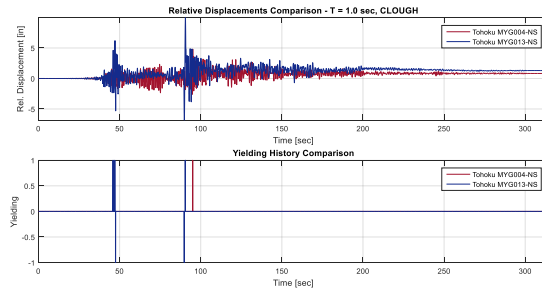*Figure 12.22. Hysteresis loop for Bilinear SDOF at 1.0 sec.*

Figure 13.23. Acceleration and yielding time history for Clough SDOF at 0.2 sec.
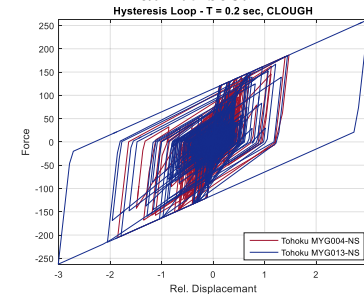
Figure 14. Hysteresis loop for Clough SDOF at 0.2 sec.

Figure 15. Acceleration and yielding time history for Clough SDOF at 1.0 sec.
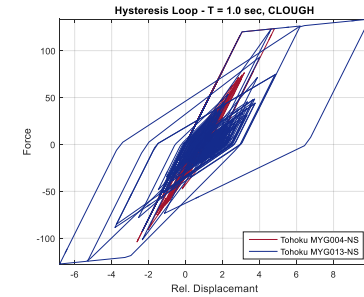
Figure 16. Hysteresis loop for Clough SDOF at 1.0 sec.
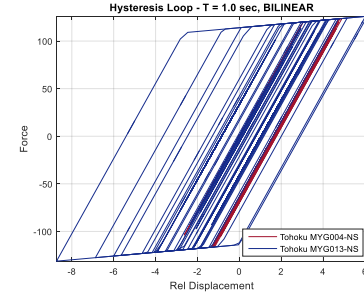
Constant strength spectra analysis

Constant strength spectra have been generated with Bispec V2 for both records. This type of spectrum considers a system with constant strength regardless its natural period. In this case, the constant strength has been represented with the coefficient C_y, which can be defined as a normalized yield capacity, F_y, defined by:

$$C_y = \frac{F_y}{W} \tag{3.1}$$

where W is the weight of the building. Two values of C_y, 0.1 and 0.3, were considered for analyses using both the Bilinear and the Clough hysteretic models. $C_y = 0.1$ is representative of low strength system, while $C_y = 0.3$ is associated with a

conventionally designed system. The results for C_y equal to 0.1 and 0.3 for the Bilinear model are shown in Figure 17.27 and corresponding results for the Clough model in Figure 3.29. The constant strength spectra obtained with the motion at Tsukidate are shown in red, while the spectra generated at Sendai are shown in blue. The bold black dashed lines in Figure 17.27 and 3.29 represent the threshold between elastic and inelastic behaviour.
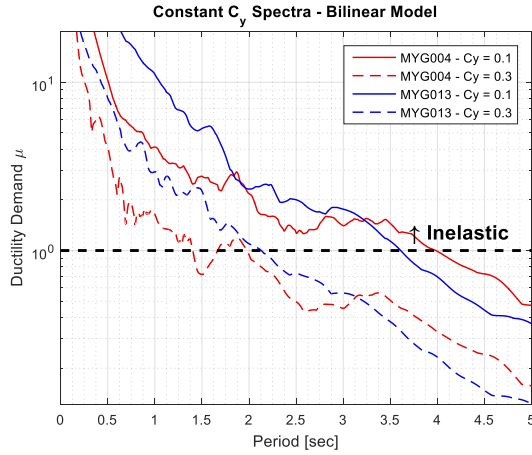

Figure 17. Constant strength spectra for Tsukidate (red) and Sendai (blue) for a Bilinear system.
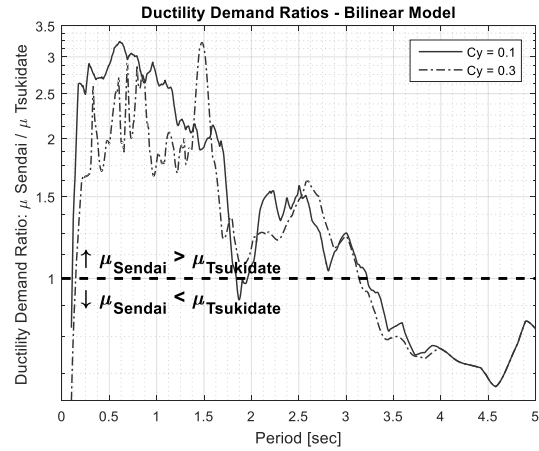

Figure 18. Spectral ratios for ductility demands for a Bilinear system.

These constant strength spectra give an indication of ductility demands, which can be directly related to the damage caused by the motions. The ductility demands imposed by the Sendai motion are consistently higher than the Tsukidate demands in the period range 0-3 sec. This means that the structural systems in this period range will be led further into the inelastic range in Sendai than in Tsukidate, provided that it has enough ductility capacity. This, in turn, implies that the structures in Sendai will experience more damage than those in Tsukidate. The conclusion holds for both the Bilinear and Clough material models and the different C_y levels. The only exception occurs at periods between 3.2 and 4.0 seconds, where the ductility demand in Tsukidate is slightly higher than the one in Sendai. However, both show ductility values lower than 2, suggesting a structural behavior close to linear elastic.

A building with fundamental period equal to 1 sec and a C_y factor equal to 0.3, is going to slightly exceed the elastic limit (ductility demand about 1.8) when subjected to the Tsukidate motion, while the ductility demand generated by the Sendai record is about 3. A building with the very same fundamental period but designed with a lower strength capacity ($C_y = 0.1$) is going to be pushed further into the inelastic range: the ductility demand at Tsukidate is about 4, while the motion in Sendai requires the structure to develop significant ductility (up to 10).
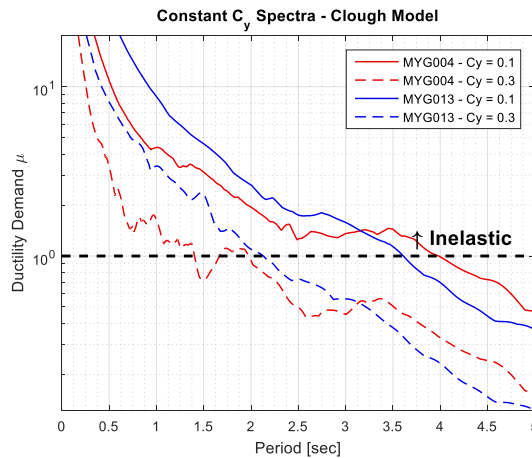

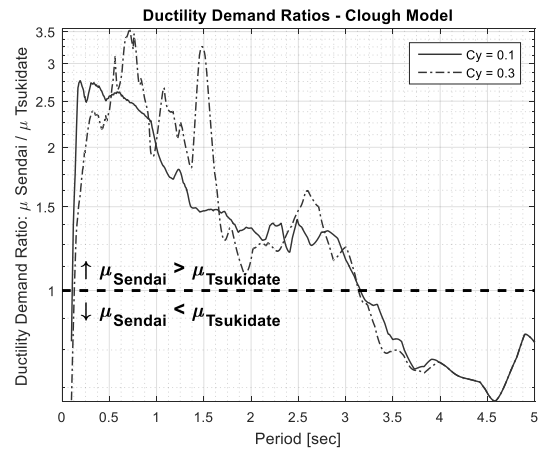*Figure 3.29. Constant strength spectra for Tsukidate (red) and Sendai (blue) for a Clough system.*

Figure 3.40. Spectral ratios for ductility demands for a Clough system.

The constant strength spectra can be interpreted also in terms of variation in the ductility demands with respect to different strength levels. As an example, let us consider Figure 17.27. The ductility demands generated by the Tsukidate motion are represented by a red solid line for weak systems ($C_y = 0.1$) and by a red dashed line for conventionally designed systems ($C_y = 0.3$). Comparing the values along the vertical ordinate, it can be inferred that weaker systems ($C_y = 0.1$) have greater displacement demands compared to stronger systems ($C_y = 0.3$). The plot also shows how for weaker systems a broader part of the spectrum (i.e. a wider range of structures) is expected to develop inelastic deformations in comparison to a stronger system. This is quite understandable, as a weaker structural system would be expected to suffer greater deformations to withstand the energy imparted by the motion in comparison to the very same motion exciting a stronger system.

Figure 18 and Figure .40 give the spectral ratios of the ductility demand at Sendai to the one at Tsukidate. Therefore, these plots provide information on the relative damage potential of the two records in terms of ductility demands. These plots confirm how the ductility demands and hence the damage to the bilinear and Clough system, are greater in Sendai than Tsukidate up to a period of 3.0 sec. In particular, in the low and intermediate period range (from 0.2 to 1.5 sec), the ductility demands at Sendai reach values up to three times higher than the ones at Tsukidate.

These findings are validated by the post-earthquake observations that the buildings that experienced damaged by the earthquake shaking in Sendai had periods in the range 0.2 to 3 sec. The relative difference of the ductility demands at the two sites decreases for period range between 1.5 and 3.2 sec, where the displacement demands in Sendai are still higher than the ones in Tsukidate, but with less significant relative difference (about 1.5 times greater).

Discussion

The relationship between structural damage and associated shaking parameters has been investigated for motions recorded during the 2011 Tohoku earthquake at the station in Tsukidate and Sendai. Peak responses such as PGA, PGV, SD and frequency contents were first considered for comparison. These parameters did not fully explain the damage potential of this type of ground motions. This finding supports the conclusions presented by previous researchers on the suitability of peak ground motion parameters to reflect the damage potential of ground motions [22, 23, 24]. The Arias intensity was found to be poorly related to the structural damage observed at the two stations in Japan, which is in contrast to other studies that show the Arias Intensity has an overall good correlation with the damage potential of ground motions from crustal earthquakes [25, 26, 27]. Moreover, contrarily to what has been demonstrated by previous studies [25,26, 24], elastic response spectra and constant ductility spectra provided only limited information about the structural demands and the associated damage. In particular, the very sharp peak with high elastic acceleration demands at Tsukidate is a poor indicator of damage. Even for a limited amount of ductility in the system, the spectral demands are drastically reduced. The constant strength spectrum showed to be consistently related to the damage potential of the earthquake motions, showing that the ductility demands at Sendai were consistently larger than at Tsukidate over a wide period range (0.15-3.2 sec). Useful information can be also obtained by the ratios between constant strength spectra ordinates, which give the relative damage potential of two different earthquake motions.

4. BEHAVIOUR OF WOOD-FRAME BUILDINGS

Over 90% of all residential buildings in North America are of wood-frame construction [28]. According to the 2016 Census of Canada [29], there were approximately 1.9 million households in the province of British Columbia (BC). About 44% (830,660) of these residential units are single-family homes and 42% (793,045) are apartment or condominium units. Low-rise light-frame wood structures consist of wood shearwalls and horizontal diaphragm components. The lateral loads induced by wind and earthquake are mainly resisted by the shear deformation of wall elements and the ductile sheathing-to-framing connections.

Historically, woodframe construction has performed quite well during earthquakes as it is flexible, light-weight, and its numerous connections and load paths could provide high ductility and absorb large amounts of earthquake input energy. As late as the 1970s, woodframe constructions were considered to be very safe in earthquakes and the existing building code was confidently believed to be sufficient [30]. However, a great number of wood houses have experienced significant damage and even collapsed during subduction events with long duration excitations [31]. Although, major efforts have been devoted to investigate the seismic resistance of timber structures since the 1994 Northridge and the 1995 Kobe earthquakes, including a series of experimental tests and the development of timber design guidelines, the issue of long duration of subduction earthquakes was not addressed explicitly [32-35].

The timber industry in North America has been actively promoting the use of wood materials for mid-rise buildings in recent years. Five- and six-story mid-rise woodframe buildings have proven popular among developers, architects, and contractors,

who see them as a cost-effective and sustainable alternative to other materials. In 2009, the British Columbia Building Code (BCBC) in Canada [36] officially permitted six-story woodframe residential buildings after a comprehensive consultation process. Three years later, the International Building Code (IBC) [37] also amended the height limit of woodframe buildings to six-stories. In 2019, the government of BCBC will allow the construction of tall wood buildings up to 12 storeys high — up from the current allowance of six. To date, more than 300 mid-rise woodframe buildings have been completed or are underway in North America, and the number is increasing. However, most of them were designed without taking ground motion duration into account.

This section describes the performance of timber structures under long duration subduction earthquakes. The investigation is confined to conventional low-rise and modern mid-rise woodframe buildings. Full scale models of the benchmark structures used for this investigation were also constructed and tested on shake tables. Three-dimensional numerical models of the structures were developed using the Timber3D program and validated with the shake table test data. To isolate the effects of duration, two sets of records that had approximately the same response spectra but different durations were selected from crustal and subduction earthquakes and used for nonlinear dynamic analyses of the model structures. Their collapse capacity was evaluated using fragility curves developed by incremental dynamic analysis.

Model Development

The low-rise light-frame wood houses studied are four two-story residential houses, which were designed per the NBCC with no seismic provisions for southwestern BC and tested at shake table at full-scale as part of the Earthquake-99 project at the University of British Columbia (UBC) [38], including: 1) Type-1 has blocked shearwalls with OSB panels, exterior stucco sheathing, and interior GWB sheathing; 2) Type-2 has blocked shearwalls with OSB panels and interior GWB sheathing only; 3) Type-3 has unblocked shearwalls with OSB panels and interior GWB sheathing, and 4) Type-4 has horizontal boards with interior GWB sheathing. All the four houses had same plan dimensions of 6.1m by 7.6m (20ft by 25ft) and storey height of 2.4m (8ft). The mid-rise building is a six-story multi-unit woodframe structure, which was designed using the simplified direct displacement design (DDD) procedure developed within the NEESWood project [41]. The building has a plan dimension of 18.1 m by 12.2 m, and a total height of 17.1 m with 2.7 m clear storey height for the first floor and 2.4 m for the upper five floors. Figure 4.1 shows the constructed buildings on the UBC and Miki shake tables.
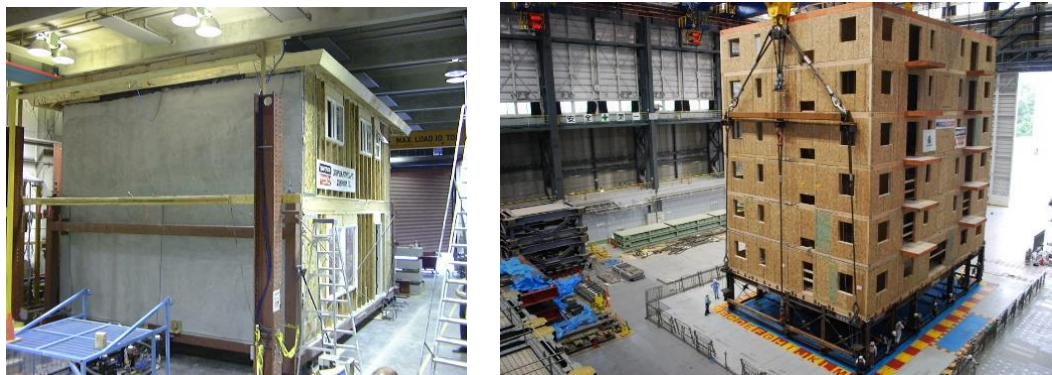
Figure 4.1. Photograph of Type-2 house and NEESWood building at full-scale shake table

In this study, a state-of-the-art three-dimensional computer program, Timber3D, originally developed within the NEES-Soft Project [33], is adopted to model the prototype buildings. Timber3D is a MATLAB-based package that simulates the nonlinear behavior and collapse of light-frame structures. It implements a nodal condensation technique to balance the computational overhead and model accuracy. The program is developed using a corotational formulation and large deformation theory. Both the in-plane and out-of-plane motions of the diaphragms under strong shaking can be modeled appropriately [39]. Figure 4.2 shows the 3D computational model of the prototype buildings developed in Timber3D.

Figure 4.2. Computational models in Timber3D. (a) low-rise house. (b) mid-rise woodframe

Incremental Dynamic Analyses

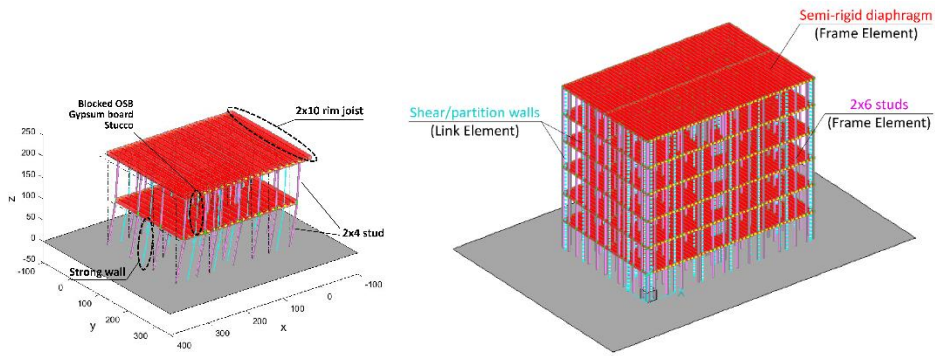The seismic response of the woodframes were evaluated by means of an incremental dynamic analysis (IDA) by using the "spectrally equivalent" ground motion suites to get the fragility curves for different seismic intensity level. In IDA, the same ground motion was scaled to multiple levels of intensity to approach collapse with respect to the spectral acceleration at the fundamental period of the woodframes [40]. In each analysis, the maximum inter-story drift ratio (IDR) was monitored as the engineering demand parameter.

Figure 4.3 presents the IDA curves of the mid-rise woodframe model for both crustal and subduction long duration motions. Overall, the median response is similar until intensity level with spectral acceleration of 2g for both types of earthquakes. Especially, the woodframe building performs quite well at the MCE design level (spectral acceleration of 1.5g) and meets the design objectives under both sets of ground motions. The maximum IDRs are all below the 3.5% drift limit as per the code requirements. This simulation result is in accord with the shake table test data [42]. However, with the increase of intensity, long duration motions seem to induce larger IDRs than the short duration motions, leading to the structural collapse at a smaller spectral acceleration. It is concluded that under long duration motions, the building obviously exhibits a lower safety margin against collapse. Similar results were also found for the four low-rise wood houses.

To further quantify the collapse rate of the building for both sets of ground excitations, the collapse fragility curves were derived from the IDA results. The fragility curves are constructed assuming a lognormal distribution.
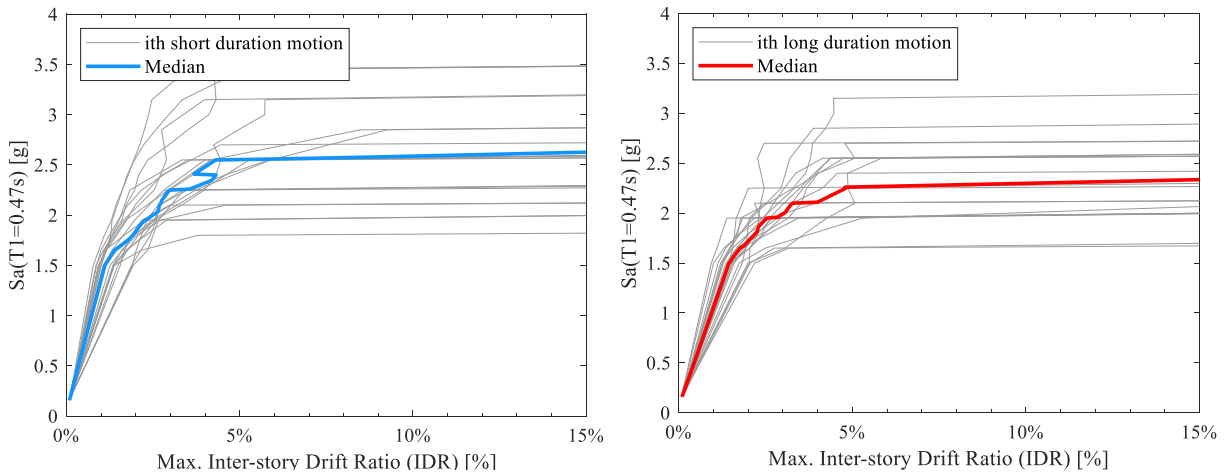
Figure 4.3. IDA curves under both sets of motions. (a) crustal motions. (b) subduction motions

Figure 4.4 shows the collapse fragility curves for the mid-rise woodframe and the Type-1 house with blocked OSB and GWB/stucco sheathing. It can be seen clearly that the buildings have low probabilities of collapse under both long and short duration motions at design intensity level. However, with the increase of intensity, the structure starts to exhibit a higher probability of collapse under long duration motions. This trend is observed within a broad range of intensity level (until spectral acceleration of 3.5g and 8g). The median collapse capacity, defined as the spectral acceleration at 50% probability of collapse, is reduced by over 18% and 26% under long duration shaking compared with that under short duration motions for both

structures. Similar observations are found for Type-2 and Type-3 houses, and especially, the collapse capacity of Type-4 houses with horizontal board sheathing is reduced by 61% under long duration shaking.

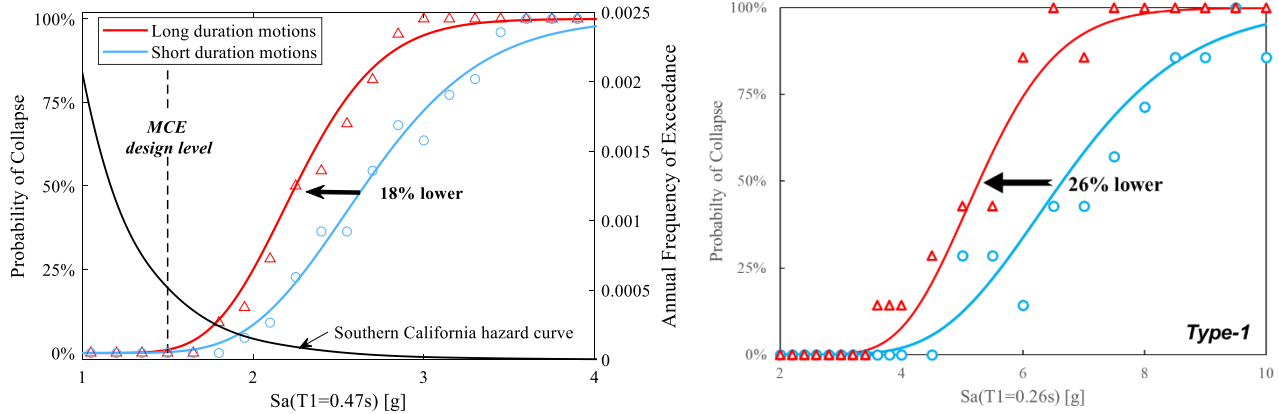*Figure 4.4. Collapse fragility curves. (a) mid-rise woodframe. (b) Type-1 house*

Damage Assessment

Recent studies on timber structures have shown that displacement alone may not be a reliable and accurate indicator for seismic performance of wood structures [42]. It was suggested that a damage-based criterion that accounts for both displacement (or ductility) and energy demands is more suitable for wood structures. In this study, the widely used Park and Ang damage index [43] is selected to evaluate the effects of ground motion duration on three wood houses at design level because of its simplicity and effectiveness. The Park and Ang damage index was originally proposed by Park and Ang (1985) for reinforced concrete buildings. This index linearly combines the maximum deformation and dissipated hysteretic energy. The equation for a single wall component can be written as:

$$DI_{wall} = \frac{\delta_m}{\delta_u} + \frac{\beta}{F_y \times \delta_u} \int dE \qquad (4.1)$$

Once the damage index is computed from each wall element, the index for the entire woodframe building can be determined by weighting the individual assemblies based on the dissipated hysteretic energy during the dynamic analysis. An IDA-based calibration process was developed recently by Liang et al. [44] and validated with experimental test results to better calibrate the β parameter. Similar to the damage states proposed for reinforced concrete structures, Liang et al. [44] also proposed damage limit states and the corresponding damage descriptions, as summarized in Table 4.1.

Table 4.1. Relationship between DI and observed damage

DI range	Damage Level	Description
DI>1.0	Collapse	Total or partial collapse
0.7<DI<1.0	Severe	Partial or complete failure of any structural component; severe cracks in walls; separation of sheathing from studs
0.4<DI<0.7	Moderate	Extensive cracking in walls, permanent deflection or near failure in structural component, severe damage of non-structural walls
0.25<DI<0.4	Minor	Hairline cracks in non-structural walls
DI<0.25	None	No visible damage

Figure 4.5 presents the estimated damage indices of the woodframe building for all 22 long and 22 short duration motions. A strong correlation of damage index with duration was observed. The median damage index under short duration motions was 0.39, which was 36% lower than the value under long duration motions (0.53). Based on the performance criteria in Table 4, the woodframe building was deemed to experience "Minor" to "Moderate" damage during short duration shaking, as the main structural components were essentially undamaged and only cracks in non-structural walls occurred. The simulation results were supported by the NEESWood shake table test report [41]. For the low-rise wood houses, it was found that system damage indices were weakly correlated with ground motion duration for Type-1 house, moderately correlated with Type-2 and3 houses, and strongly correlated with Type-4 house at design intensity level.
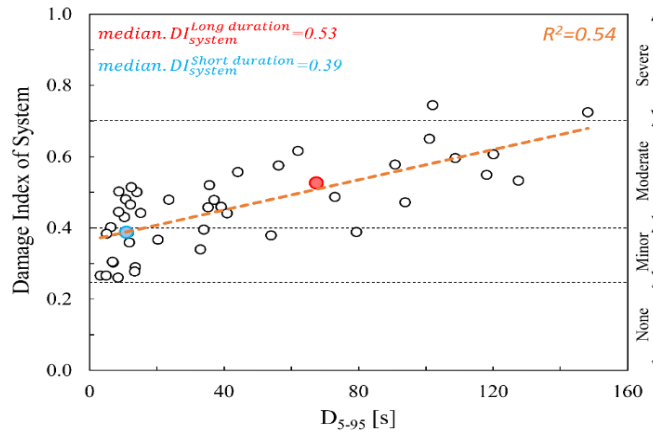
Figure 4.5. Correlation of system damage index with duration for mid-rise woodframe

Experimental Studies of light frame wood structures

This sections discusses the use of numerical models to predict the seismic behaviour of light-frame wood structures subjected to long duration ground motions. Results of shake table test of a full-scale wood frame classroom were used for this investigation. First, a highly detailed numerical model of the test structure was created. The nails, framing members, hold-downs and sheathing were modeled explicitly and the contributions of the strength and stiffness around wall openings and non-structural sheathing was included. Time-history analysis results from the model were directly compared to the full-scale test data to validate the models. The tests comprised running the shake table for short and long duration ground motion records such as those obtained from the 1995 Kobe, Japan event and 1971 San Fernando event (short duration) and the 2011 Tohoku, Japan event (long duration), at different intensity levels. To best perform the comparison a spectrally equivalent short duration motion was selected for the long duration motion. An experiential and analytical study was then completed with spectrally equivalent pairs.

During the test program, the structure was subject to extreme levels of shaking which induced large drift levels up to and exceeding 6% drift. The test data are used to examine the capability of numerical models to predict the damage of wood frame structure near collapse subjected to high intensity ground motions. Also, the effect of non-structural sheathing and the strength and stiffness contributions of the openings are investigated. The validated detailed model was then used to investigate the effect of the duration of ground motions on the performance of light-frame wood structures. An image of the full-scale test setup is shown in Figure 4.6.
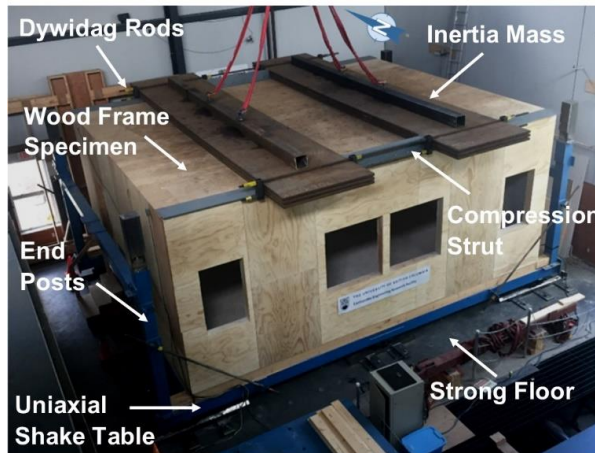
Figure 4.6. Full-Scale Test Setup

Numerical Model

The prediction for the wall behavior was completed using a detailed M-CASHEW2 model (Figure 4.7). The M-CASHEW model, developed by Pang and Hassenzadeh [45], is a 2D shear wall and diaphragm modeling program. The frame elements have four translational and two rotational degrees of freedom (DOF). The sheathing panels are modeled with one rotational DOF, two translational DOFs and two shear DOFs. The bending and axial elongation of the framing members, separation and

bearing contacts between framing members, uplift and anchorage of the hold down devices, shear deformation of the sheathing panels, nonlinear shear slip response of the sheathing nails, and second order effect of gravity loads (P-delta) can be captured.

Figure 4.7. M-CASHEW Model of Classroom North and South Elevation for Second Testing Configuration

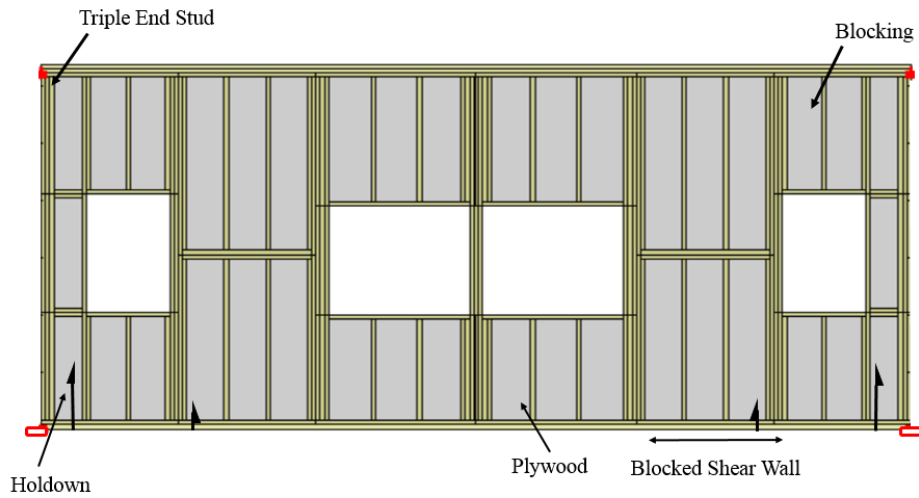Several connection types are defined in a database available in the M-CASHEW program and have been used for the classroom wall model. The sheathing nails between the framing and the plywood were modelled with the evolutionary parameter hysteretic model, EPHM material model fitted to the connection test data by Ekiert and Hong [46] for nominal 51mm (2 in.) thick Hem-Fir attached to 11.1 (7/16 in.) thick OSB using 8d common nails. This data was available and the difference in the sheathing type was felt to not significantly affect the response. The EPHM model was developed to capture the behaviour of light-frame wood shear walls at high drift levels where stiffness and strength degradation is significant. In-cyclic and cyclic deterioration of strength and stiffness is included in the model, which according to Ibarra et al. [47] and Chandramohan et al. [3] makes the model suitable for studying the influence of duration of ground motion on collapse.

The gypsum sheathing and framing connections are modeled with the MSTEW material model based on cyclic tests by Dinehart et al. [48] of No. 6 gypsum screws and 12mm (1/2 in.) thick gypsum wall board. The frame-to-frame shear slip for the double stud nails are modeled elastically. The end nail connections between the end posts and sill plates were modelled with a non-linear hold-down spring to describe the uplift response and nail withdrawal, as well as a M-STEW model to described the shear-
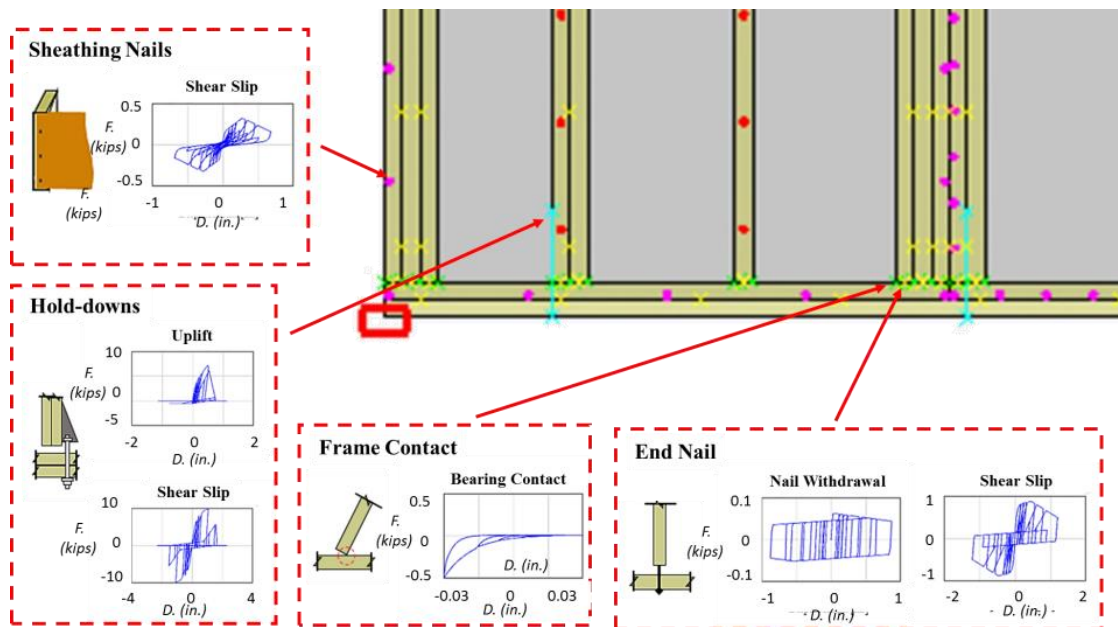

Figure 4.8. Hysteretic models for frame contact, end nails, sheathing nails, and PHD5 Hold-downs, [49]

slip response of two 10d sinker nails. A non-linear contact element is used to describe the bearing deformation between the framing elements. The hold-down elements were modelled with non-linear hold-down springs based on the component testing by United Steel Products (UPS) hold-downs and matched by van de Lindt et al. [49]. The details of the components of the model and the hysteretic material models in M-CASHEW numerical model used are shown in Figure 4.8.

It should be noted that the elements were tested using the CUREe protocol [50]. This protocol has been recognised to be realistic for simulating earthquake loading effects for light-frame wood construction. This protocol better captures the effect of crustal ground motions, further investigation of the effect on behaviour of the elements with longer protocols with multiple pulses should be completed to have a better representation of the element behavior in a long duration seismic event.

Comparison of Numerical Model and Experimental Result

The response spectra and time history for the short duration and long duration spectrally equivalent pairs are shown in Figure 4.9 for the KOBE_KAK090/ Tohoku_MYG0161103111446-EW records. The ground motions were scaled to the 2% in 50 years' interface subduction hazard level for Victoria, BC.
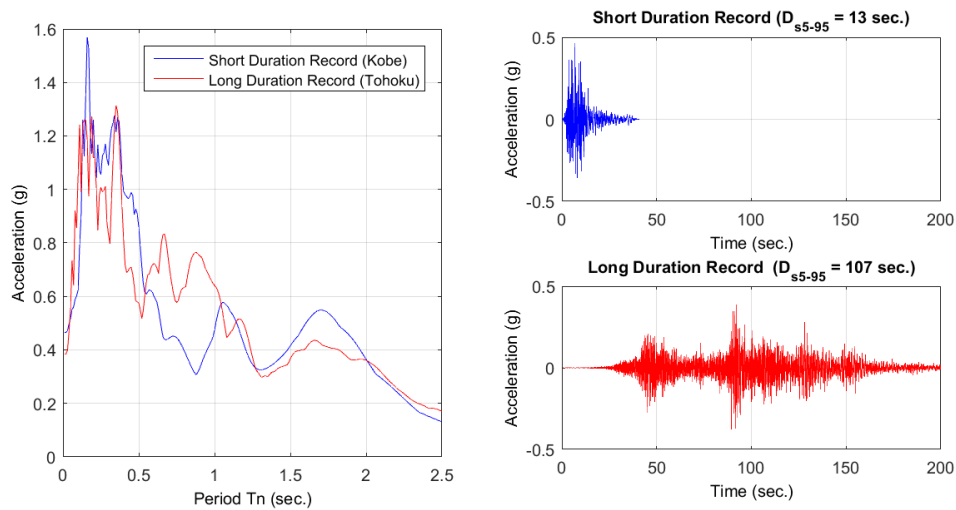

Figure 4.9. Kobe and Tohoku spectrally equivalent records (a) response spectra and (b) time history of short and long duration records
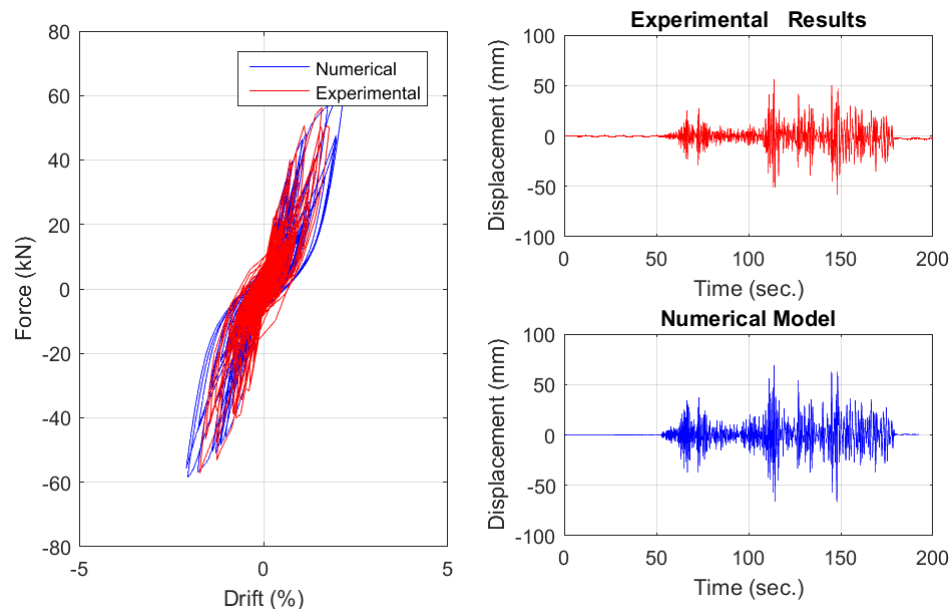

Figure 4.10. Numerical Model and Experimental (a) hysteresis (b) displacement time history for Long Duration Run 1
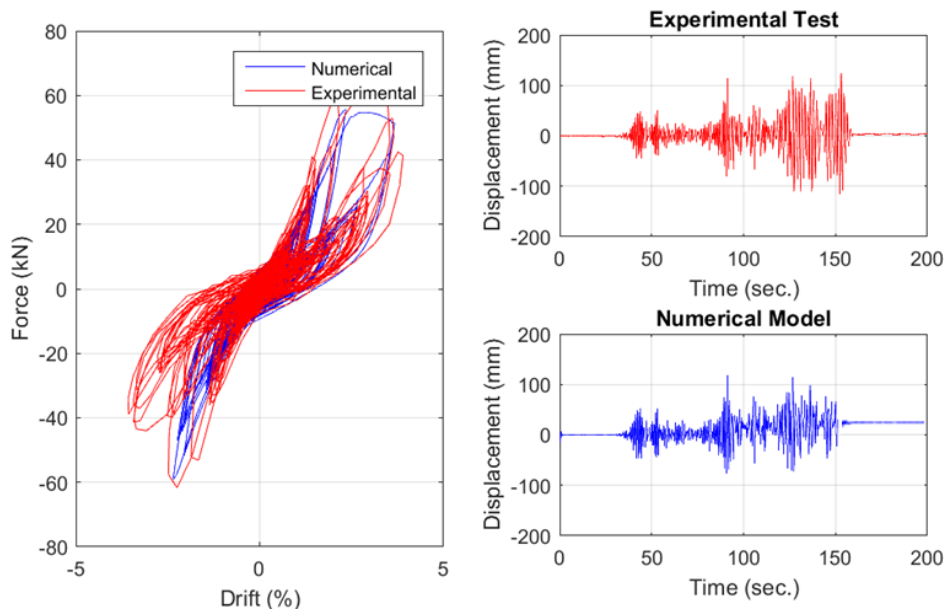
Figure 4.11. Numerical Model and Experimental (a) hysteresis (b) displacement time history for Long Duration Run 2

During the experimental tests, the specimen experienced drifts between 1%-2% for the first run. At this damage level the gypsum board cracked along window corners and some nail tear through occurred. Failure of the shear walls was localized along the edges of the panel. During the second run the specimens experienced drifts up to 4%. The dominant mode of failure in the shear walls was nail pull through and localized shear off of nails. The residual drift of the specimen was close to zero and the specimen carried the full internal loads after the tests.

The comparison of the numerical and experimental displacement time-history and hysteretic response for two consecutive runs for the long duration motion, respectively, are shown in Figure 4.10 and Figure 4.11. The time-history response of the model and test specimen show close to the same dynamic behaviour. The hysteretic damping seems to match reasonably well. Overall, it was observed that the long duration motion caused the specimen and model to experience more drift and damage.

A comparison of the force-drift hysteretic and time-history response of analysis using the validated MCASHEW model for additional long and short duration ground motions pairs is shown in Figure 4.12 and Figure 4.13. At the design hazard level, the long duration ground motion caused 32% and 27% more drift than the first and second especially equivalent short duration motion, respectively. This suggests that the margin against collapse may be lower when this type of system is subjected to long duration motions. A more comprehensive analysis program should be completed with a wider selection of various ground motions scaled to a range of hazard levels to have a better characterize of the effect of ground motion duration on seismic behaviour and expected collapse.

Discussion

The effects of long duration subduction earthquakes include a reduction of the median collapse capacities of both conventional low-rise and modern mid-rise woodframe structures significantly. Specifically, the reduction was 18% for the mid-rise woodframe building, and as high as 61% for the low-rise woodframe with horizontal board sheathing. The quantification of duration effects depends on the level of ground shaking and damage measure used. At the design intensity level, the use of drift may not be adequate to characterize the effects of duration. The use of a cumulative Park and Ang damage index would result in a different assessment and showed that long duration subduction motion does have a significant effect on performance.

A full-scale wood frame classroom was tested on the linear shake table at the UBC EERF facility. The testing program was performed to evaluate the effect ground motion duration on the seismic performance of light-frame wood structures. The full-scale classroom was subjected a series of ground motions. A detail numerical model (M-CASHEW2) where each nail, stud, sheathing panel, and hold-down was modeled explicitly was built. hysteretic and time-history response of the structure was accurately predicted for the first two runs. The results suggested that for spectrally equivalent short duration and long duration ground motion pairs the structure would experience more damage and higher absolute drift during a long duration seismic event. Fairhurst et. al. [51] and Chandramohan et al. [52] concluded similar trends for conventionally constructed reinforced concrete coupled shearwall buildings.
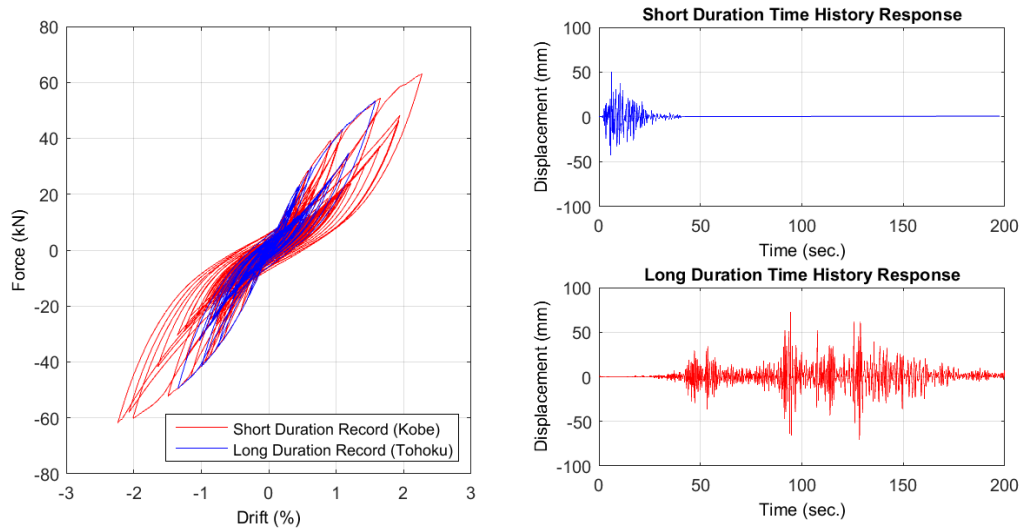
Figure 4.12. Comparison of numerical analysis results for Kobe (Short) and Tohoku (Long) spectrally equivalent ground motions (a) hysteresis, (b) displacement time-history
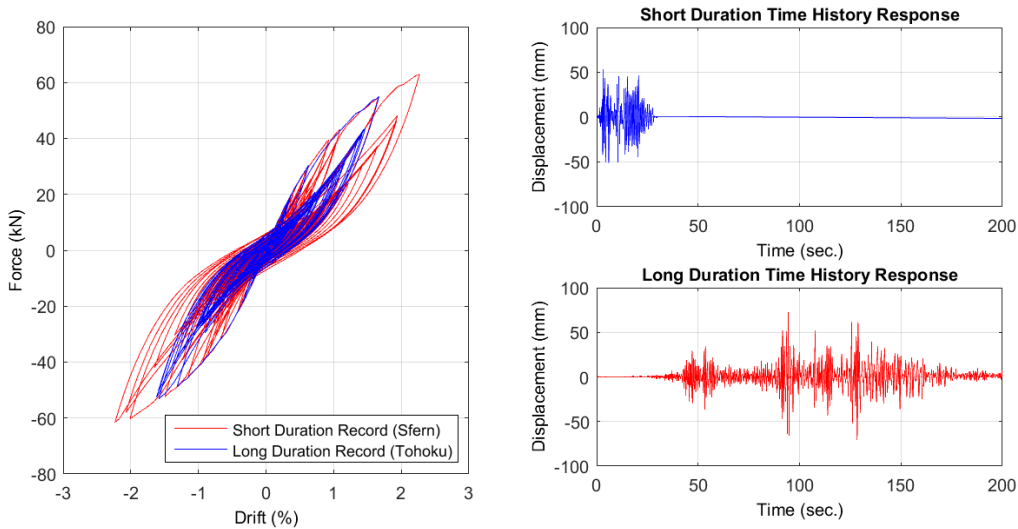

Figure 4.13. Comparison of numerical analysis results for San Fernando (Short) and Tohoku (Long) spectrally equivalent ground motions (a) hysteresis, (b) displacement time-history

5. BEHAVIOUR OF CONCRETE BUILDINGS

In this section, the effect of ground motion duration on reinforced concrete (RC) concrete shearwall buildings is investigated. The archetype buildings in this study are RC shearwall buildings typical of residential buildings constructed in Vancouver, British Columbia (BC), Canada (a large city with a dense urban population in close proximity to the Cascadia Subduction Zone). Buildings with 6, 12, 18, 24, and 30 stories are considered. Cyclic and in-cycle degradation is accounted for in the coupling beam models as well as the material models used in fiber sections of the shearwalls. Two suites of spectrally equivalent records are run at various levels of shaking, up to the collapse level, in order to determine if the collapse risk of the structure is influenced by ground motion duration.

Model Development

A typical floor plan of the modeled buildings floor plan is illustrated in Figure 5-1a. The lateral load resisting system includes three interior reinforced concrete shearwalls which comprise the elevator and stair core of the building. The gravity resisting system of the building includes circular perimeter and interior columns and 8" slabs at each story. The floor area is about 5200 ft^2 per story and the weight was calculated as 0.21 kips/ft^2 (approximately 10 kN/m^2).

19

The buildings were designed using the equivalent lateral force procedure (ELFP) for a base shear calculated in accordance with the 2010 National Building Code of Canada (NBCC) for Vancouver, BC based on conventionally constructed coupled walls [53]. The seismic force reduction factor (R_dR_o) of this system is 1.95. Reinforcement in the 18 story building shearwalls is illustrated in Figure 5-1b. The walls are coupled by 2' deep header beams which are reinforced by transverse 15M stirrups spaced at 4".
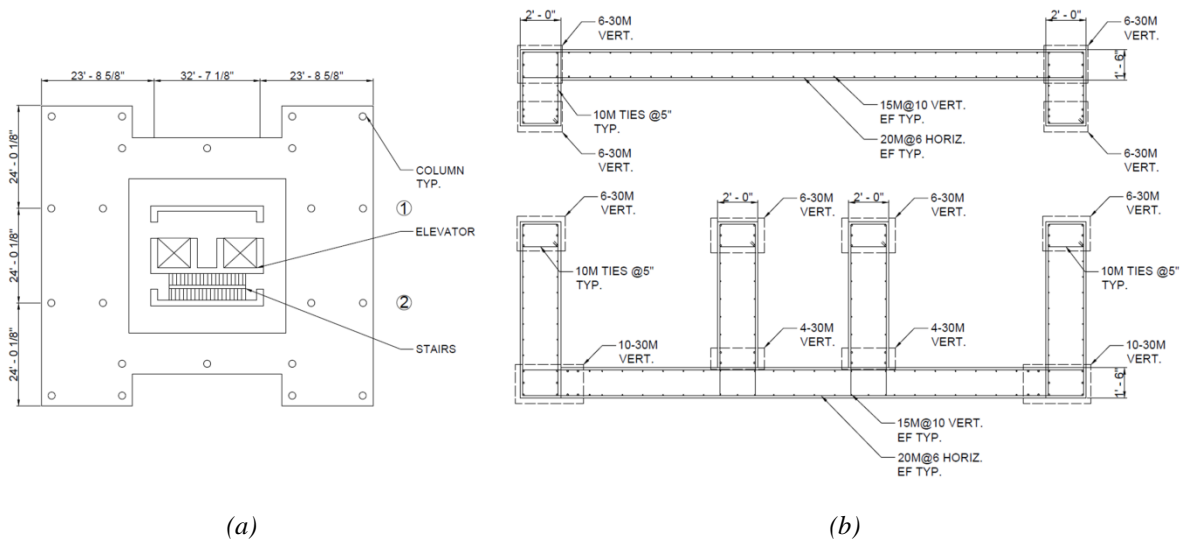

(a)   *(b)*

Figure 5.1. Archetype building (a) floor plan, and (b) shearwall reinforcement

The OpenSees framework [54] was used to develop a numerical model for the archetype buildings following Fairhurst et al. [51]. The header beams were modeled using elastic beam elements to with nonlinear shear hinges to account for the shear yielding and nonlinearity in the elements. The elastic beam elements were modeled considering a cracked section modulus ($I_{cracked} = 0.35I_{gross}$) [55]. The nonlinear shear hinge properties were calibrated to a reverse-cyclic test on a similar beam performed by Galano and Vignoli [56] using the Pinching4 material model [57]. This model is able to capture pinching, in-cycle degradation, and cyclic stiffness and strength degradation. A comparison of the test results to the calibrated Pinching4 material model is presented in Figure 5-2a.

The interior shearwalls were modeled using fiber elements with a displacement-based formulation and elastic shear hinges to capture elastic shear deformations. The elastic shear hinges had a stiffness reduced to 0.1 times their elastic stiffness to account for cracking.

Concrete was modeled using the Concrete02 material model in OpenSees [58]. Confinement was accounted for using the Mander et al. relationship [59]. Both crushing and spalling are captured in this material model. Reinforcing steel was modeled using the ReinforcingSteel material model which can account for cyclic fatigue [60]. Buckling and fracture of the reinforcement was captured through the use of the MinMax material. To do this, the MinMax material was set to return zero strength and stiffness when the strain in the steel material reached the concrete crushing strain (assuming steel buckling will occur immediately after the surrounding concrete crushes) or the steel fracture strain [61].

To account for the second order effects of the weight carried by the gravity system a leaning (or P-Delta) column was included in the model. The weight of the structure not applied directly on the shearwalls was applied on the leaning column. Rigid diaphragm constraints were applied at each level.

Damping was applied as 2.5% Rayleigh damping in the first and third modes. The first mode periods of the models (from 6 to 30 stories) were 0.44, 1.05, 1.74, 2.56, and 3.73 s, respectively. An illustration of the OpenSees models is presented in Figure 5-2b.
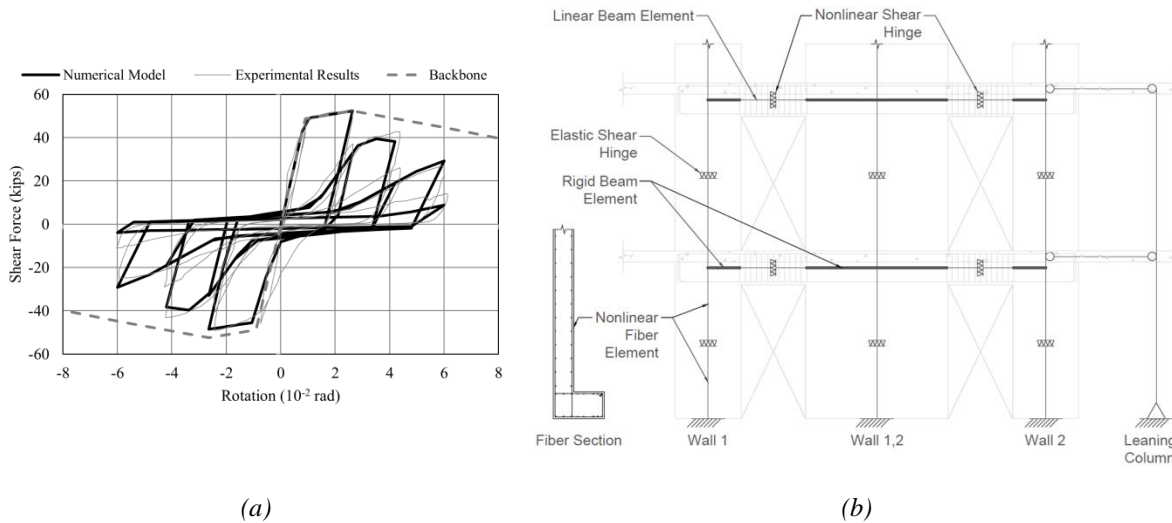
(a)   (b)

Figure 5.2. (a) Nonlinear shear hinge model for the header beams, and (b) typical storey of the OpenSees model

Incremental Dynamic Analyses

Ground motion suites

Two suites of 30 ground motion records were selected in order to investigate the effect of ground motion duration on the archetype building models. The NGA-West2 database [62] was used to select shallow crustal events; the COSMOS [63] and K-Net [64] databases were used to download subduction interface events from worldwide and Japanese events, respectively. The first suite of motions contained long duration records, while the second comprised spectrally equivalent short duration records. The 5-95% significant duration ($D_{5\text{-}95}$) was adopted to quantify record duration. $D_{5\text{-}95}$ refers to the time between the accumulations of 5% to 95% of the total Arias intensity of the record. Significant duration has been noted in previous studies to be well correlated to collapse capacity ratio (the ratio of collapse to design shaking level) and damage in structures [3, 4].

First, 30 long duration records ($D_{5\text{-}95} > 35$ s) were selected and linearly scaled to the Vancouver 2% in 50 year spectrum. Most of the events are from large magnitude subduction interface and crustal events. For this study, spectral shape and significant duration were the most important aspects of the records, thus, no selection constraints, other than limiting initial scale factors to the design spectrum to 4.0, were employed in order to maximize the number of records available. This limit was applied to both record suites.
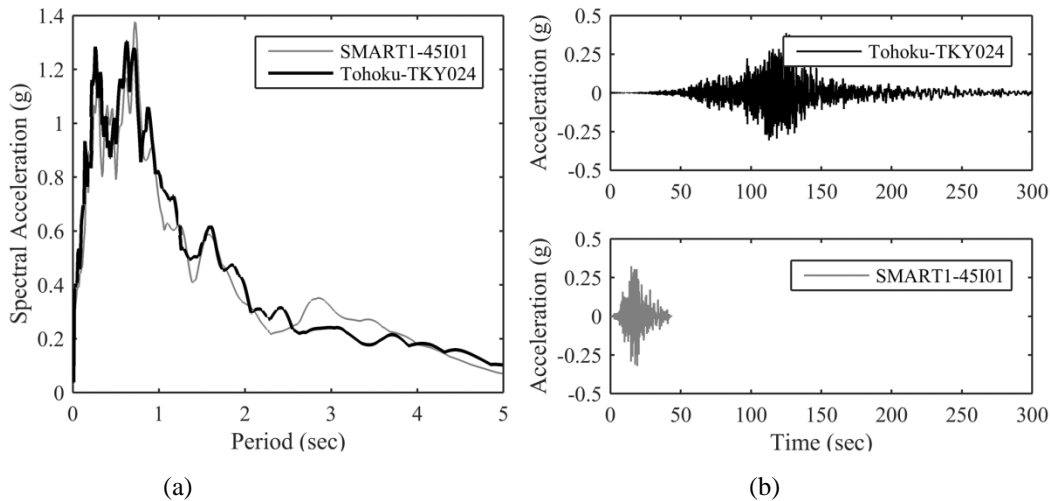

(a)   (b)

Figure 5.3. Example of spectrally equivalent records: (a) 5% damped response spectra and (b) acceleration time histories

The methodology proposed by Chandramohan et al. [3] was then used to select spectrally equivalent short duration motions. This methodology removes the influence of spectral shape so that the effect of duration can more easily be isolated. Accordingly, a short duration ($D_{5-95} < 20sec$) record was selected to best match the spectrum of each of the 30 long duration records. The best match was obtained by minimizing the mean squared error (MSE) between the spectra of the two records. Scaling factors and MSE was computed between 0.07-5.6sec, which is equal to 0.15 times the 6 story model's period to 1.5 times the 30 story model's period. Figure 5.3 illustrates an example of a long record and spectrally equivalent short duration record.

Figure 5.4 presents the spectra of the two suites compared to the Vancouver 2015 design spectrum. The short duration suite comprised records with a 5-95% significant durations of 5 to 15 s with a mean of 11 s. The long duration suite had a range of 40 to 150 s and a mean of 80 s.
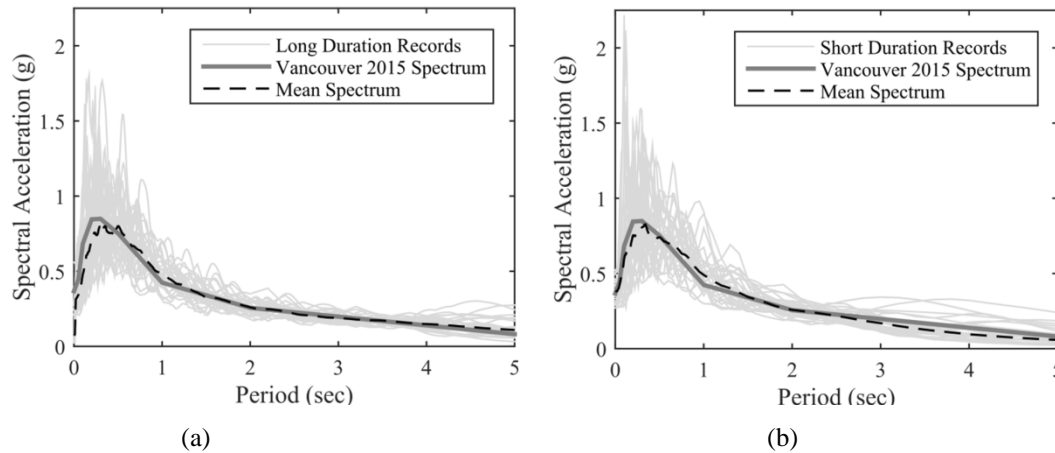

(a)   (b)

Figure 5.4. Spectra of (a) the long duration suite and (b) the short duration suite compared to the Vancouver 2% in 50 year design spectrum

Collapse analysis

In order to determine if long duration ground motions increase the collapse risk of reinforced concrete shearwall structures at higher shaking levels, the two suites of ground motions were incrementally scaled up until collapse was reached. Collapse is defined in this study as excessive interstory drifts (>5%). This drift limit was chosen because the gravity system; which was not explicitly modeled, but idealized as a single leaning column; is not expected perform past 5% drift. This is also slightly over the allowable maximum drift limit from LATBSDC of 4.5% [55] and past the point where the incremental dynamic analysis (IDA) curves became flat. Other forms of non-simulated collapse, including shear demands in the walls were checked, but did not govern.

Figure 5.5 presents the empirical and lognormal fragility curves derived for the 6 story building model for the two ground motion suites. In this figure the 100% scaling level refers to the 2% in 50 year shaking level (the code design level according to the NBCC). Note that the 2% in 50 year shaking level is computed with contributions from both crustal and subduction ground motions. The same reference level was considered for both suites (as opposed to using a 2% in 50 year shaking level computed for each individual source) because the object of this study was to compare the effect of short and long duration motions – not crustal vs. subduction ground motions.

For the 6 story model the median collapse levels for the long and short suites are 146% and 190% of the design scaling level, respectively. The median collapse scaling levels for the other archetype models are summarized in Table 5.1. The short duration suite consistently requires scaling levels ~10-30% higher than those required for the long duration suite to induce collapse. The minimum required increase in collapse scaling level is 8% for the 30 story model, while the maximum is 30% for the 6 story model. This makes sense considering the 6 story model has a much lower period compared to the 30 story model, meaning it will undergo more cycles during the motions and will accumulate more inelastic damage, increasing the difference between the two record suites.

Table 5.1. Mean collapse scaling level for all archetype models

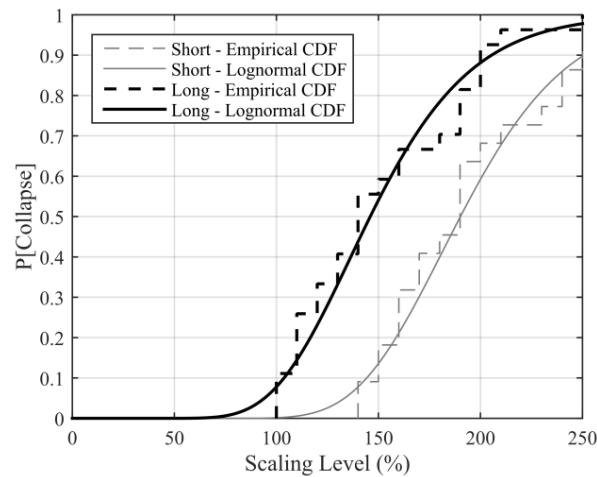| Number of Stories	Median Collapse Scaling Level (% of 2% in 50 year level)		
	Long Duration Suite	Short Duration Suite	Short/Long
6	146	190	1.30
12	136	166	1.22
18	146	189	1.29
24	174	201	1.16
30	198	214	1.08
Average	160	192	1.21

Figure 5.5. CDF results for the long and short duration suites for the 6 story model

Discussion

A suite of reinforced concrete shearwall buildings was analyzed using two sets of records: a long duration suite, and a spectrally equivalent short duration suite. When the ground motion records were incrementally scaled to very high levels of shaking using IDA, the median collapse scaling level of the models was significantly affected by ground motion duration. The short duration suite, on average, required scaling factors 20% greater than the long duration suite in order to induce structural collapse (as indicated by large drift values). The differences between the two suites are more exaggerated for the shorter building models.

This implies that when considering larger levels of shaking, where large levels of damage are expected - e.g. to determine the safety of structures - then duration becomes an essential parameter of the input motions for this type of structure. The observation that ground motion duration can significantly affect the median collapse scaling level of structures is in line with the conclusions of other recent studies conducted using moment resisting frames [2,3,52].

6. CONCLUSIONS

1) This paper explored how different characteristics of subduction ground motions affect damage potential. The relationship between the observed structural damage and associated shaking intensities was investigated for motions recorded during the 2011 Tohoku earthquake (Tsukidate and Sendai station). Several characteristics have been considered for comparison. PGA has been shown not to be a good index for structural damage potential. The Arias intensity was found to be poorly correlated to the structural damage observed at the two stations. Elastic response spectra and constant ductility spectra were generated for the two ground motions under consideration but they provided only limited information about the structural demands and the associated damage. In particular, the very sharp peak

characterizing the elastic acceleration demands at Tsukidate is a poor indicator of damage. The implementation of constant strength spectra indicated that the relative damage potential of the Tsukidate and Sendai ground motions can be explained more fully. These spectra provide the ductility demand imposed by a given ground motion on a variety of systems with different fundamental periods and for two specific constant strength conditions. The analysis of the constant strength spectra showed that the ductility demands (hence, deformation demands) at Sendai were consistently larger than at Tsukidate over a wide period range (0.15-3.2 sec).

Hancock and Bommer [66] provide a comprehensive state-of-knowledge review on the effect of ground motion duration on structural damage. In their review they note that most studies using cumulative damage or displacement measures find a correlation between ground motion duration and structural damage. However, studies that use extreme responses (such as maximum interstorey drift or displacement) generally do not find correlations between duration and damage. This, however, may be to a lack of cyclic degradation in the models employed in many of these studies. Additionally, most of the experimental tests reviewed showed a high degree of relevance of ground motion duration and number of cycles on specimen damage.

2) There has been little research in determining the effect of duration and subduction earthquakes on wood structures. In this paper, experimental and numerical studies have been presented to investigate the effect of the duration of ground motions on the performance and probability of collapse of light-frame wood structures, as well as to have a better prediction of the response of the structure in a subduction earthquake with a large magnitude (Mw ~ 9). The effects of long duration subduction earthquakes on the computational models of both low-rise and modern mid-rise woodframe buildings were evaluated in this study. Long duration motions reduced the median collapse capacities of both conventional low-rise and modern mid-rise woodframe structures significantly. Specifically, the reduction was 18% for the mid-rise woodframe building, and as high as 61% for the low-rise woodframe with horizontal board sheathing. The quantification of duration effects depends on the level of ground shaking and damage measure used. At the design intensity level, the use of drift may not be adequate to characterize the effects of duration. The use of cumulative Park and Ang damage index would result in a different assessment and showed long duration subduction motion does have a significant effect on performance. The findings and results of this study help current seismic design practice gain a better understanding of the effects of ground motion duration and provide information essential for improving the seismic design of timber structures.

A full-scale wood frame classroom was tested on the linear shake table at the UBC EERF facility. The testing program was performed to evaluate the effect ground motion duration on the seismic performance of light-frame wood structures. The full-scale classroom was subjected a series of ground motions. A detail numerical model (M-CASHEW2) where each nail, stud, sheathing panel, and hold-down was modeled explicitly was built. hysteretic and time-history response of the structure was accurately predicted for the first two runs. The results suggested that for spectrally equivalent short duration and long duration ground motion pairs the structure would experience more damage and higher absolute drift during a long duration seismic event.

3) The behaviour of reinforced concrete shearwall buildings was analyzed using two sets of records: a long duration suite, and a spectrally equivalent short duration suite. When the ground motion records were incrementally scaled to very high levels of shaking using IDA, the median collapse scaling level of the models was significantly affected by ground motion duration. The short duration suite, on average, required scaling factors 20% greater than the long duration suite in order to induce structural collapse (as indicated by large drift values). The differences between the two suites are more exaggerated for the shorter building models. This implies that when considering larger levels of shaking, where large levels of damage are expected - e.g. to determine the safety of structures - then duration becomes an essential parameter of the input motions for this type of structure.

ACKNOWLEDGMENTS

REFERENCES

[1] Chopra, A. K. (2016). *Dynamics of Structures: Theory and Applications to Earthquake Engineering.* (5th ed.). Upper Saddle River, New Jersey, USA: Pearson Prentice Hall.

[2] Raghunandan, M., & Liel, A. B. (2013). Effect of ground motion duration on earthquake-induced structural collapse. *Structural Safety, 41*, 119-133.

[3] Chandramohan, R., Baker, J. W., & Deierlein, G. G. (2016). Quantifying the influence of ground motion duration on structural collapse capacity using spectrally equivalent records. *Earthquake Spectra, 32*(2), 927-950.

[4] Fairhurst, M., Bebamzadeh, A., & Ventura, C. E. (2017). Collapse risk of tall concrete shearwall buildings under long duration ground motions. *Los Angeles Tall Buildings Structural Design Council Conference*, (p. 14). Los Angeles.

[5] Campillo, M., Gariel, J., Aki, K., & Sanchez-Sesma, F. (1989, December). Destructive Strong Ground Motion in Mexico City: Source, Path and Site Effects During Great 1985 Michoan Earthquake. *Bullettin of the Seismological Society of America, 79*(6), 1718-1735.

[6] Wirgin, A., & Bard, P.-Y. (1996). Effects of Buildings on the Duration and Amplitude of Ground Motion in Mexico City. *Bullettin of Seismological Society of America, 86*(3), 914-920.

[7] Shearer, P., & Burgmann, R. (2010). Lessons Learned from the 2004 Sumatra-Andaman Megathrust Rupture. *Annual Review of Earth and Planetary Sciences*(38), pp. 103-31.

[8] Saatcioglu, M., Ghobarah, A., & Nistor, I. (2006). Performance of Structures in Indonesia during the December 2004 Great Sumatra Earthquake and Indian Ocean Tsunami. *Earthquake Spectra, 22*(S3), S295-S319.

[9] Cluff, L. S. (2008). Effects of the 2004 Sumatra-Andaman Earthquake and Indian Ocean Tsunami in Aceh Province. *The Bridge, 37*(1), pp. 12-16. Retrieved from https://www.nae.edu/File.aspx?id=7405&v=70df971

[10] Kaushik, H. B., & Jain, S. K. (2007). Impact of Great December 26, 2004 Sumatra Earthquake and Tsunami on Structures in Port Blair. *Journal of Performance of Constructed Facilities*, 128-142.

[11] GEER Association. (2010). Geo-Engineering Reconnaissance of the 2010 Maule, Chile Earthquake.

[12] Elnashai, A. S., Genturk, B., Kwon, O.-S., Al-Qadi, I. L., Hashash, Y., Roesler, J. R., Valdivia, A. (2010). *The Maule (Chile) Earthquake of February 27, 2010.* Mid-America Earthquake Center.

[13] USGS. (2012). *20 Largest Earthquakes in the World*. Retrieved December 10, 2017, from Earthquake List, Maps & Statistics: https://earthquake.usgs.gov/earthquakes/browse/largest-world.php

[14] Shojiro, K., Kazuhiro, N., Kazunari, M., & Masahiro, K. (2011). Strong Mootion and Earthquake Response Records of the 2011 off the Pacific Coast of Tohoku Earthquake. *43rd Joint Meeting of U.S.-Japan Panel on Wind and Seismic Effects.* Tsukuba, Japan: Public Works Research Institute.

[15] Nishiyama, I., Okawa, I., Fukuyama, H., & Okuda, Y. (2011). Building Damage by the 2011 off the Pacific coast of Tohoku earthquake and coping activities by NILIM and BRI collaborated with the administration. *43rd Joint Meeting of U.S.-Japan Panel on Wind and Seismic Effects.* Tsukuba, Japan: Public Works Research Institute.

[16] Japan Meteorological Agency. (2017). *Tables explaining the JMA Seismic Intensity Scale*. Retrieved July 4, 2017, from http://www.jma.go.jp/jma/en/Activities/inttable.html#ryuui

[17] Ochi, S., & Suzuoki, M. (2011). The lessons of the Great East Japan Earthquake 2011 and the countermeasures against earthquakes and tsunamis in future - Fundamental Concepts behind Future Tsunami Disaster Prevention. *43rd Joint Meeting of U.S.-Japan Panel on Wing and Seismic Effects.* Tsukuba, Japan: Public Works Research Institute.

[18] National Research Institute for Earth Science and Disaster Prevention (NIED). (2017). Strong-motion seismograph networks (K-NET, Kik-net). Japan: National Research Institute for Earth and Disaster Resilience. Retrieved July 6, 2017, from http://www.kyoshin.bosai.go.jp/

[19] Scott, M. H., & Mason, H. B. (2017). Constant-ductility response spectra for sequential earthquake and tsunami loading. *Earthquake Engineering and Structural Dynamics*.

[20] Earthquake Solutions. (2017). *Providing State-of-the-Art Software for Structural and Earthquake Engineering*. Retrieved July 4, 2017, from Bispec 2.20: http://www.eqsols.com/Pages/Bispec.aspx

[21] Clough, R. (1966). *Effect of stiffness degradation on earthquake ductility requirements.* University of California, Department of Civil Engineering, Berkeley.

[22] Elenas, A. (2011). Intensity parameters as damage potential descriptors of earthquakes. In M. Papadrakakis, M. Fragiadakis, & V. Plevris (Ed.), *Proceedings of the 3rd International Conference on Computational Methods in Structural Dynamics and Earthquake Engieering. 26*, pp. 327-334. Corfu, Greece: Springer, Dordrecht. doi:10.1007/978-94-007-5134-7_19

[23] Cantagallo, C., Camata, G., Spacone, E., & Corotis, R. (2012). The variability of deformation demand with ground motion intensity. *Probabilistic Engineering Mechanics, 28*, 59-65. doi:10.1016/j.probengmech.2011.08.016

[24] Kadas, K., & Yakut, A. (2014). Correlation of seismic demands with ground motion intensity parameters evaluated through different ground motion record sets. *Proceedings of the 10th U.S. National Conference on Earthquake Engineering.* Anchorage, Alaska.

[25] Elenas, A. (2000). Correlation between seismic acceleration parameters and overall structural damage indices of buildings. *Soil Dynamics and Earthquake Engineering, 20*(1-4), 93-100. doi:10.1016/S0267-7261(00)00041-5

[26] Elenas, A., Lioios, A., Vasiliadis, L., Sakellari, M., & Koliopoulos, P. (2001). A numerical estimation of the interrelation between acceleration parameters and damage indicators in earthquake engineering. In E. Aifantis, & A. N. Kounadis (Ed.),

Proceedings of the 6th National Congress of Mechanics. I, pp. 254-260. Thessaloniki, Greece: Hellenic Society of Theoretical and Applied Mechanics.

[27] Nanos, N., Elenas, A., & Ponterosso, P. (2008). Correlation of different strong motion duration parameters and damage indicators of reinforced concrete structures. *Proceedings of the 14th World Conference on Earthquake Engineering.* Beijing, China.

[28] Ayoub, A. (2007). "*Seismic analysis of wood building structures*". Engineering Structures, 2007. **29**(2): p. 213-223.

[29] Canada, S. (2016). *2016 Census Profile of British Columbia [online]*. [cited 2019 Feb 25]; Available from: https://www.statcan.gc.ca/eng/start.

[30] Li, Y. and Ellingwood, B.R. (2007) "*Reliability of woodframe residential construction subjected to earthquakes*". Structural Safety, **29**(4): p. 294-307.

[31] Goda, K. and Salami, M.R. (2014) "*Inelastic seismic demand estimation of wood-frame houses subjected to mainshock-aftershock sequences*". Bulletin of Earthquake Engineering, **12**(2): p. 855-874.

[32] Filiatrault, A., Fischer, D., Folz, B., Uang, C. M. (2002). "*Seismic testing of two-story woodframe house: Influence of wall finish materials*". Journal of Structural Engineering, **128**(10): p. 1337-1345.

[33] Pang, W., E. Ziaei, and Filiatrault, A. (2012). "A 3D model for collapse analysis of soft-story light-frame wood buildings". *Proc. of 12th World Conference on Timber Engineering*, Auckland, New Zealand.

[34] Pei, S. and van de Lindt, J. (2011). "*Seismic numerical modeling of a six-story light-frame wood building: Comparison with experiments*". Journal of Earthquake Engineering, **15**(6): p. 924-941.

[35] Tomasi, R., Sartori, T., Casagrande, D., Piazza, M. (2015). "*Shaking Table Testing of a Full-Scale Prefabricated Three-Story Timber-Frame Building*". Journal of Earthquake Engineering, **19**(3): p. 505-534.

[36] Ministry of Housing and Social Development (2009). *Regulation of the Minister of Housing and Social Development*, Ministerial Order No. M008, Province of British Columbia. Victoria, British Columbia, Canada.

[37] IBC (2012). *International Code Council.* International Building Code. International Code Council: Washington DC, United States.

[38] White, T. and Ventura, C.E. (2006). *Seismic Performance of Wood-frame Residential Construction in British Columbia*, Earthquake Engineering Research Facility, p. 46 pages.

[39] Pang, W. and Hassanzadeh Shirazi, S.M. (2012). "*Corotational model for cyclic analysis of light-frame wood shear walls and diaphragms*". ASCE Journal of Structural Engineering, **139**(8): p. 1303-1317.

[40] Vamvatsikos, D. and Cornell, C.A. (2002). "*Incremental dynamic analysis*". Earthquake Engineering & Structural Dynamics, **31**(3): p. 491-514.

[41] Pei, S., van de Lindt, J. W., Pryor, S. E., Shimizu, H., Isoda, H. (2010). *Seismic testing of a full-scale six-story light-frame wood building: NEESWood Capstone test*, in NEESWood Report NW-04.

[42] Park, S. and van de Lindt, J. (2009). "*Formulation of seismic fragilities for a wood-frame building based on visually determined damage indexes*". Journal of Performance of Constructed Facilities, **23**(5): p. 346-352.

[43] Park, Y.-J. and Ang, A.H-S. (1985). "*Mechanistic seismic damage model for reinforced concrete*". ASCE Journal of Structural Engineering, **111**(4): p. 722-739.

[44] Liang, H., Wen, Y.K., Foliente, G.C. (2010). "*Damage modeling and damage limit state criterion for wood-frame buildings subjected to seismic loads.* ASCE Journal of Structural Engineering, **137**(1): p. 41-48.

[45] Pang, W. and Hassanzadeh, M. (2010). "Next generation numerical model for non-linear in-plane analysis of wood-frame shear walls". *In World Conference on Timber Engineering*, Trento Province, Italy., 2010.

[46] Ekiert, C. and Hong, J. (2006). "Framing-to-Sheathing Connection Tests in Support of NEESWood Project". Network of Earthquake Engineering Simulation Host Institution: State University of New York at University at Buffalo, Buffalo, NY.

[47] Ibarra, L., Medina, R. and Krawinkler, H. (2005). "Hysteretic models that incorporate strength and stiffness deterioration". Earthquake Engineering & Structural Dynamics, 34(12), 1489-1511

[48] Dinehart, D. W., Blasetti, A. S., and Shenton III, H. W. (2008). "Experimental cyclic performance of viscoelastic gypsum connections and shear walls". Journal of Structural Engineering, 134(1), 87-95.

[49] van de Lindt, J. W., Pei, S., Pang, W., and Shirazi, S. M. H. (2011). "Collapse testing and analysis of a light-frame wood garage wall". Journal of Structural Engineering, 138(4), 492-501.

[50] CUREe.(1998). CUREe-Caltech Woodframe Project Newsletter. Retrieved from http://www.curee.org/projects/woodframe/.

[51] Fairhurst, M., Bebamzadeh, A. and Ventura, C. (2019). "Effect of Ground Motion Duration on Reinforced Concrete Shear Wall Buildings". Earthquake Spectra, 35(1), 311-331.

[52] Chandramohan, R., Baker, J. W., and Deierlein, G. G. (2016). "Impact of hazard-consistent ground motion duration in structural collapse risk assessment". Earthquake Engineering & Structural Dynamics, 45(8), 1357-1379.

[53] National Research Council of Canada - NRCC (2010). *National Buildings Code of Canada*, Ottawa, Ont., Canada.

[54] McKenna, F., Fenves, G.L., Scott, M.H. & Jeremic, B. (2000). *Open System for Earthquake Engineering (OpenSees)*, Pacific Earthquake Engineering Research Center, Berkely, Ca.

[55] Los Angeles Tall Building Structural Design Council - LATBSDC (2017). *An Alternative Procedure for Seismic Analysis and Design of Tall Buildings Located in the Los Angeles Region*. Los Angeles, Ca.

[56] Galano, L. & Vignoli, A. (2000). "Seismic behavior of short coupling beams with different reinforcement layouts". *ACI Structural Journal* 97(6), 876-885.

[57] Lowes, L.N., Mitra, N. & Altoontash, A. (2004). *A Beam-column Joint Model for Simulating the Earthquake Response of Reinforced Concrete Frames, PEER Report 2003/10.* Pacific Earthquake Engineering Center (PEER), University of California, Berkeley, Ca.

[58] Yassin, M.H.M. (1994). *Nonlinear Analysis of Prestressed Concrete Structures under Monotonic and Cyclic Loads*, Doctoral Dissertation, University of California, Berkeley, Ca.

[59] Mander, J.B., Priestley, M.J. & Park, R. (1988). "Theoretical stress-strain model for confined concrete". *Journal of Structural Engineering*, 114(8), 1804-1826.

[60] Brown, J. & Kunnath, S.K. (2000). *Low Cycle Fatigue Behavior of Longitudinal Reinforcement in Reinforced Concrete Bridge Columns, NCEER Technical Report 00-0007*, National Center for Earthquake Engineering Research, State University of New York at Buffalo, Buffalo, N.Y.

[61] Pugh, J. (2012). *Numerical Simulation of Walls and Seismic Design Recommendations for Walled Buildings*, Doctoral Dissertation, University of Washington, Seattle, Wa.

[62] Ancheta, T.D., Darragh, R.B., Stewart, J.P., Seyhan, E., Silva, W.J., Chiou, B.S., & Kishida, T. (2013). *Peer NGA-West2 database*. Pacific Earthquake Engineering Research Center (PEER), Berkeley, Ca.

[63] The Consortium of Organizations for Strong-Motion Observation Systems - COSMOS. *Strong-motion Virtual Data Center (VDC).* Available at: http://www.strongmotioncenter.org.

[64] Kinoshita, S. (1998). Kyoshin Net (K-net), *Seismological Research Letters*, 69(4), 309-332.

[65] Hancock, J., & Bommer, J.J. (2006). A state-of-knowledge review of the influence of strong-motion duration on structural damage. *Earthquake Spectra*, 22(3), 827-845.